

CrystEngComm

Accepted Manuscript



This is an *Accepted Manuscript*, which has been through the Royal Society of Chemistry peer review process and has been accepted for publication.

Accepted Manuscripts are published online shortly after acceptance, before technical editing, formatting and proof reading. Using this free service, authors can make their results available to the community, in citable form, before we publish the edited article. We will replace this *Accepted Manuscript* with the edited and formatted *Advance Article* as soon as it is available.

You can find more information about *Accepted Manuscripts* in the [Information for Authors](#).

Please note that technical editing may introduce minor changes to the text and/or graphics, which may alter content. The journal's standard [Terms & Conditions](#) and the [Ethical guidelines](#) still apply. In no event shall the Royal Society of Chemistry be held responsible for any errors or omissions in this *Accepted Manuscript* or any consequences arising from the use of any information it contains.

Zinc and cadmium metal-directed coordination polymers: in situ flexible tetrazole ligand synthesis, structures, and properties

Ruoting Dong, Yingzhao Ma, Xinli Chen, Lanfen Huang, Qianhong Li, Mingyuan Hu, Moyuan Shen, Chuwen Li, Hong Deng*

School of Chemistry & Environment and Guangzhou Key Laboratory of Materials for Energy Conversion and Storage, Guangzhou 510006, PR China

To whom correspondence should be addressed. E-mail: dh@scnu.edu.cn

ABSTRACT

Seven zinc and cadmium coordination frameworks, $\{[\text{Zn}_2(\text{TE})_2] \cdot \text{H}_2\text{O}\}$ (**1a**); $\{[\text{Cd}_2(\text{TE})(\text{SO}_4)(\text{OH})(\text{H}_2\text{O})]\}$ (**1b**); TE = 2-(1H-Tetrazol-5-yl)-ethanol, $\{[\text{Zn}_{1.5}(\text{TA})(\text{INA})] \cdot 4\text{H}_2\text{O}\}$ (**2a**); $\{[\text{Cd}_{4.5}(\text{TA})_3(\text{N}_3)(\text{OH})_2(\text{H}_2\text{O})_2] \cdot \text{H}_2\text{O}\}$ (**2b**); $\{[\text{Zn}(\text{MT})(\text{INA})] \cdot \text{H}_2\text{O}\}$ (**2c**); TA = (1H-Tetrazol-5-yl)-acetic acid, MT = 5-methyl-tetrazole, INA = isonicotinic acid, $\{[\text{Cd}(\text{BTMA})] \cdot \text{H}_2\text{O}\}$ (**3a**); $[\text{Cd}_2(\text{TTMA})(\text{OH})]$ (**3b**); BTMA = bis-(1H-tetrazol-5-ylmethyl)-amine; TTMA = tris-(1H-tetrazol-5-ylmethyl)-amine, were obtained through *in situ* tetrazole synthesis and have been structurally characterized by single crystal and powder X-ray diffraction, as well as elemental analyses, FT-IR spectroscopy and thermal studies. Interestingly, by varying the reaction conditions of hydrothermal synthesis, the unprecedented *in situ* generation of TA and MT for **2** based on cyanoacetamide or BTMA and TTMA for **3** based on iminodiacetonitrile was observed, respectively. Compound **1a** represents a very interesting example of three-dimensional (3D) frameworks containing hexagonal channels and meso-helical chains (P + M) alternately trapped by Zn-TE coordination interactions; Compound **1b** possesses a two-dimensional (2D) layered structure constructed from infinite organic chains and sulfate anions. Compounds **2a** and **2b** both crystallize in 3D frameworks containing infinite rod-shaped SBUs; Compound **2c** displays a two-fold diamondoid network constructed by the interconnection of Zn-MT-INA honeycomb layers and INA ligands. Compound **3a** shows a 3D framework consisting of cyclic $[\text{Cd}_2(\text{BTMA})_2]$ dimer subunits, possessing a 8-connected network topology. Compound **3b** shows a 3D binodal (4,8)-connected net based on tetranuclear $[\text{Cd}_4\text{O}_2]$ polyoxometalates (POMs) as nodes. Furthermore, the luminescent properties of these compounds were investigated. Notably, compound **1b** crystallizes in an acentric space group representing significant second harmonic generation (SHG) efficiencies.

Introduction

Over the past decades, extensive attention has been paid to the design and synthesis of the metal-organic hybrid compounds due to their fascinating structural properties and potential applications in fluorescence, catalysis, magnetism, molecular recognition, and enantioselective separation.¹⁻² Crystal engineering based on coordination polymer is an efficient strategy for designing and synthesizing metal-organic frameworks (MOFs) with elegant topologies and potential applications. The tetrazole possessing four nitrogen atoms have been extensively utilized in coordination chemistry.³ 5-substituted-1H-tetrazole are among the most important and popular species used to construct MOFs.⁴⁻⁵ It is a landmark breakthrough that Demko and Sharpless pioneered a safe, convenient and environmentally friendly synthetic method for the synthesis of 5-substituted 1H-tetrazoles derivatives *via* a [2+3] cycloaddition reaction of azide anions and nitriles in water with the aid of Lewis acid as a catalyst.⁶ With the development of this method, a variety of such *in situ* generated 5-R-tetrazoles (R=alkyl,⁷ pyrazinyl,⁸ pyrimidyl,⁹ pyridyl,¹⁰ phenyl,¹¹ amino,¹² etc.) have been employed as excellent chelating and/or bridging ligands to construct novel metal coordination polymers, which were not only found to possess intriguing architectures as well as potential applications as functional materials, but also confirmed the significance of the selection of organic linkers in the assembly of MOFs as well.¹³ In our previous work, novel tetrazole frameworks have been successfully *in situ* synthesized by tuning the organic ligands.¹⁴

Among the reported 5-R-tetrazole-related *in situ* synthesis examples, it is often the case that the ligand components generally retain the structural integrity, and intensive effort has been reported trying to approach structural and property diversities by varying the nitriles, which in turn give different 5-R-tetrazole ligands.^{9-11,15} However, during our previous exploration of the coordination compounds based on MT (MT = 5-methyl-tetrazole), we have observed that the MT was unexpectedly generated *via* the *in situ* hydrothermal decarboxylation reaction of cyanoacetic acid and NaN_3 .^{14a} This has encouraged us to explore the coordination chemistry with nitriles which may not retain the structural integrity in hydrothermal *in situ* metal-catalyzed reaction and thus to form unexpected 5-R-tetrazole ligands. In other words,, under proper conditions, the significant structure transformation may be realized by tuning *in situ* generated ligands, however, from the same nitriles. An extended literature survey shows that, few such efforts utilizing the same nitriles under different reaction conditions have been carried out so far. While some unique hydrothermal reactions may occur that involves *in situ* hydrolysis,¹⁶ carbon-carbon coupling,¹⁷ cleavage and

formation of disulfide bonds,¹⁸ and decarboxylation of aromatic groups,¹⁹ etc.²⁰ In light of this, we were intrigued by the possibility of using same precursors that would allow unique hydrothermal reactions approaching the *in situ* generation of disparate tetrazole ligands to alter the structures of compounds.

Based on the above considerations and as part of our ongoing efforts in the design and synthesis of tetrazole-based MOFs,^{14,21} we chose herein 3-hydroxy-propionitrile, cyanoacetamide and iminodiacetonitrile, sodium azide with different Zn(II) and Cd(II) salts as catalysts to synthesize novel metal-organic coordination frameworks for several considerations: (1) The d¹⁰ zinc and cadmium metal cation not only are able to tolerate various coordination numbers and geometries, but also exhibit luminescent properties when bound to functional ligands;^{22,14a} (2) their expected *in situ* generated ligands can exhibit excellent coordination capacities with five, six and eight coordination sites of tetrazolate rings and O donors; (3) as we all know, cyanoacetamide contains an amide group which can be easily hydrolyzed under the condition of heating for a long time,²³ and iminodiacetonitrile containing two cyan groups can be very active in nucleophilic reactions and susceptible to nucleophilic attack.²⁴ This prompted us to select cyanoacetamide and iminodiacetonitrile as potential sources for the formation of unexpected tetrazolate ligands by varying reaction conditions; (4) the presence of $-\text{CH}_2-\text{CH}_2-\text{OH}$, $-\text{CH}_2-\text{COOH}$ and $-\text{CH}_2-\text{NH}-\text{CH}_2-$ groups offers flexible orientations, thus the conformational freedom may better satisfy the geometric requirement for metal ions to construct diversified and intriguing architectures and topologies.²⁵

In this context, we report seven novel tetrazole coordination frameworks including one 2D layers and six 3D frameworks. To our knowledge, all *in situ* generated ligands have never been explored in the construction of coordination polymers, although a few coordination polymers associated with flexible 5-substituted tetrazole ligands were reported.^{26,25b-d} By varying the hydrothermal synthesis conditions we have achieved the unprecedented *in situ* generation of tetrazole ligand TA, MT both based on cyanoacetamide and BTMA, TTMA both based on iminodiacetonitrile for **2** and **3**. In particular, to the best of our knowledge, the ligand TTMA in **3b** was first prepared by hydrothermal technique involving both [2+3] cycloaddition and nucleophilic substitution as well as used for constructing coordination compounds. The thermal stabilities and the solid-state photoluminescence properties of the seven compounds and preliminary SHG investigation of **1b** are also reported.

Experimental Section

Materials and instruments

All the materials and reagents were obtained commercially and used without further purification. Elemental (C, H, N) analyses were performed on a Perkin–Elmer 2400 element analyzer. Infrared (IR) samples were prepared as KBr pellets, and spectra were obtained in the 4000–400 cm^{-1} range using a Nicolet Avatar 360 FT-IR spectrophotometer. ESI-MS spectrum was carried out on a Thermo Finnigan LCQ Deca XP Max LC/MSn instrument. Thermogravimetric analysis (TGA) experiments were carried out on a Perkin-Elmer TGA 7 thermogravimetric analyzer with the heating rate of 10 $^{\circ}\text{C}/\text{min}$ from 50 to 800 $^{\circ}\text{C}$ under dry air atmosphere. Powder XRD investigations were carried out on a Philips PW-1830 X-ray diffractometer with Cu $K\alpha$ radiation. Fluorescence spectra were recorded with an F-4600 FL spectrophotometer analyzer. The second-order nonlinear optical effect was determined on a LAB130 Pulsed Nd:YAG laser.

Synthesis of $\{[\text{Zn}_2(\text{TE})_2]\cdot\text{H}_2\text{O}\}$ (**1a**)

A mixture of ZnCl_2 (0.136 g, 1mmol), 3-hydroxy-propionitrile (2ml), and NaN_3 (0.130 g, 2 mmol) in H_2O (10 mL) was stirred for 30 min at room temperature and then sealed in a 23 mL Teflon-lined autoclave at 150 $^{\circ}\text{C}$ for 72 hours. After the mixture was cooled to room temperature at a rate of 5 $^{\circ}\text{C}/\text{h}$, colorless rod-like single crystals of **1a** were obtained (yield: 70% based on Zn). Anal. Calcd (%) for $\text{C}_{18}\text{H}_{19.98}\text{N}_{24}\text{O}_7\text{Zn}_6$: C, 20.07; H, 18.70; N, 31.22. Found: C, 20.05; H, 18.72; N, 31.17. IR data (KBr, cm^{-1}): 3650(m), 3604(w), 3433(s), 2954(w), 2900(m), 2854(m), 2375(m), 1720(s), 1579(s), 1498(m), 1318(w), 1190(m), 1073(s), 720(w), 576(w), 522(s).

Synthesis of $[\text{Cd}_2(\text{TE})(\text{SO}_4)(\text{OH})(\text{H}_2\text{O})]$ (**1b**)

A mixture of CdSO_4 (0.208 g, 1mmol), 3-hydroxy-propionitrile (2ml), and NaN_3 (0.130 g, 2 mmol) in H_2O (10 mL) was stirred for 30 min at room temperature and then sealed in a 23 mL Teflon-lined autoclave at 150 $^{\circ}\text{C}$ for 72 hours. After the mixture was cooled to room temperature at a rate of 5 $^{\circ}\text{C}/\text{h}$, yellow block single crystals of **1b** were obtained (yield: 80% based on Cd). Anal. Calcd (%) for $\text{C}_{2.56}\text{H}_7\text{Cd}_2\text{N}_4\text{O}_{7.44}\text{S}$: C, 6.55; H, 1.50; N, 11.93. Found: C, 6.57; H, 1.48; N, 11.91. IR data (KBr, cm^{-1}): 3647(w), 3421(s), 2964(w), 2340(w), 1716(m), 1604(m), 1395(m), 1282(m), 1188(s), 1111(s), 1033(s), 952(s), 859(m), 781(w), 674(m), 617(s), 497(w).

Synthesis of $\{[\text{Zn}_{1.5}(\text{TA})(\text{INA})]\cdot 4\text{H}_2\text{O}\}$ (**2a**)

A mixture of ZnCl_2 (0.136 g, 1mmol), cyanoacetic acid (0.085 g, 1mmol), isonicotinic acid (0.061 g, 0.5mmol) and NaN_3 (0.130 g, 2 mmol) in H_2O (10 mL) was stirred for 30 min at room temperature and then sealed in a 23 mL Teflon-lined autoclave at 150 $^{\circ}\text{C}$ for 72 hours. After the mixture was cooled to room temperature at a rate of 5 $^{\circ}\text{C}/\text{h}$, colorless rod-like single crystals of **2a** were obtained (yield: 80% based on Zn). Anal. Calcd (%) for $\text{C}_{18}\text{H}_{20}\text{N}_{10}\text{O}_{12}\text{Zn}_3$: C, 28.27; H, 2.64; N, 18.32.

Found: C, 28.25; H, 2.70; N, 18.29. IR data (KBr, cm^{-1}): 3394(m), 3082(m), 2991(w), 2356(w), 2079(s), 1597(s), 1573(s), 1487(w), 1442(s), 1381(m), 1250(m), 1120(w), 827(m), 763(s), 725(m).

Synthesis of $\{[\text{Cd}_{4.5}(\text{TA})_3(\text{N}_3)(\text{OH})_2(\text{H}_2\text{O})_2]\cdot\text{H}_2\text{O}\}$ (**2b**)

A mixture of $\text{Cd}(\text{NO}_3)_2\cdot 2.4\text{H}_2\text{O}$ (0.236 g, 1mmol), cyanoacetic acid (0.085 g, 1mmol) and NaN_3 (0.130 g, 2 mmol) in H_2O (10 mL) was stirred for 30 min at room temperature and then sealed in a 23 mL Teflon-lined autoclave at 150 °C for 72 hours. After the mixture was cooled to room temperature at a rate of 5°C/h, colorless rod-like single crystals of **2b** were obtained (yield: 35% based on Cd). Anal. Calcd (%) for $\text{C}_{18}\text{H}_{23.66}\text{Cd}_9\text{N}_{30}\text{O}_{21.83}$: C, 10.70; H, 1.18; N, 20.79. Found: C, 10.68; H, 1.20; N, 20.77. IR data (KBr, cm^{-1}): 3425(s), 3209(w), 2987(m), 2363(w), 2102(s), 1732(s), 1573(s), 1481(m), 1419(m), 1372(m), 1127(w), 929(m), 843(m), 705(m), 589(m).

Synthesis of $\{[\text{Zn}(\text{MT})(\text{INA})]\cdot\text{H}_2\text{O}\}$ (**2c**)

Yellow block single crystals of **2c** were obtained under similar reaction conditions as **2a**, except that the isonicotinic acid was added to 1mmol (0.123 g) (yield: 53% based on Zn). Anal. Calcd (%) for $\text{C}_8\text{H}_9\text{N}_5\text{O}_3\text{Zn}$: C, 33.29; H, 3.14; N, 24.27. Found: C, 33.27; H, 3.16; N, 24.23. IR data (KBr, cm^{-1}): 3340(s), 2971(s), 2640(w), 2356(m), 1934(w), 1557(m), 1365(m), 1220(w), 1091(s), 1049(s), 998(w), 879(s), 820(w), 712(m).

Synthesis of $\{[\text{Cd}(\text{BTMA})]\cdot\text{H}_2\text{O}\}$ (**3a**)

A mixture of $\text{CdCl}_2\cdot 2.5\text{H}_2\text{O}$ (0.228 g, 1mmol), iminodiacetonitrile (0.096 g, 1mmol), and NaN_3 (0.130 g, 2 mmol) in H_2O (10 mL) was stirred for 30 min at room temperature and then sealed in a 23 mL Teflon-lined autoclave at 150 °C for 72 hours. After the mixture was cooled to room temperature at a rate of 5°C/h, colorless rod-like single crystals of **3a** were obtained (yield: 25% based on Cd). Anal. Calcd (%) for $\text{C}_4\text{H}_5\text{CdN}_9\text{O}$: C, 15.62; H, 1.64; N, 40.99. Found: C, 15.60; H, 1.61; N, 40.95. IR data (KBr, cm^{-1}): 3631(m), 3456(m), 3339(s), 2967(w), 2916(m), 1618(s), 1500(s), 1433(s), 1352(s), 1298(s), 1239(s), 1128(m), 1083(m), 898(s), 770(m), 677(s), 524(m).

Synthesis of $[\text{Cd}_2(\text{TTMA})(\text{OH})]$ (**3b**)

A mixture of $\text{CdCl}_2\cdot 2.5\text{H}_2\text{O}$ (0.228 g, 1mmol), iminodiacetonitrile (0.096 g, 1mmol), NaN_3 (0.130 g, 2 mmol) and 2,2'-bipyridyl (0.156 g, 1 mmol) in H_2O (10 mL) was stirred for 30 min at room temperature and then sealed in a 23 mL Teflon-lined autoclave at 180 °C for 72 hours. After the mixture was cooled to room temperature at a rate of 5°C/h, colorless prismatic single crystals of **3b** were obtained (yield: 38% based on Cd). Anal. Calcd (%) for **3b**, $\text{C}_6\text{H}_7\text{Cd}_2\text{N}_{13}\text{O}$: C, 14.35; H, 1.41; N, 36.27. Found: C, 14.29; H, 1.37; N, 36.23. IR data (KBr, cm^{-1}): 3674(s), 3437(s), 2893(w), 2063(s), 1734(w), 1643(w), 1600(s), 1521(m), 1438(s), 1365(m), 1218(m), 1180(w), 1147(m), 920(w), 773(s), 673(m).

Crystal Structure Determination

Single crystal X-ray diffraction data collections of **1-3** were performed on a Bruker Apex II CCD diffractometer operating at 50 kV and 30 mA using Mo K α radiation ($\lambda = 0.71073 \text{ \AA}$) at room temperature. Data collection and reduction were performed using the APEX II software.²⁷ Multi-scan absorption corrections were applied for all the data sets using the APEX II program.²⁷ The structures were solved by direct methods and refined by full-matrix least-squares on F^2 using the SHELXL program package.²⁷ All non-hydrogen atoms were refined with anisotropic displacement parameters. Hydrogen atoms attached to carbon were placed in geometrically idealized positions and refined using a riding model. Hydrogen atoms on water molecules and nitrogen atom were located from difference Fourier maps and were also refined using a riding model. The disordered guest molecules for compounds **2a** and **3a** were removed by SQUEEZE²⁸ in structural refinement. The elemental analysis and TGA studies indicate the existence of four H₂O molecules in **2a** and one in **3a** respectively. Crystallographic data for compounds **1-3** were listed in Table 1, and selected bond lengths and angles were given in the Table S1, Supporting Information. CCDC numbers: 1040503-1040507, 901623-901624 for compounds **1-3**, respectively.

Results and Discussion

Synthesis

Hydrothermal treatment of nitriles (R-CN) and sodium azide with the aid of different zinc and cadmium salts resulted in the formation of Zn/Cd-tetrazole coordination compounds (Scheme 1). Two pairs of compounds (**1a** and **1b**, **2a** and **2b**) were successfully obtained by changing the metal ions coordinating to the tetrazole ligands, while the syntheses of **2c** were carried out under the same synthetic condition as that of **2a** except for the amount of INA. It should be noted that only the pH value is different during the preparation of **2a** and **2c**, indicating that the pH value may have an important effect on the structural assembly of zinc compounds based on cyanoacetamide. By exploitation of the *in situ* hydrothermal reactions, compound **3a** and **3b** were synthesized using the precursor iminodiacetonitrile, NaN₃ and suitable cadmium salts. In this work, there are three rather important determinants in the formation of them: one is the reaction temperature, the second is the presence of 2,2'-bipyridyl in synthesizing **3b**, and the last one is the suitable cadmium(II) salts. The reaction temperature should be kept at 170 °C and 180°C for **3a** and **3b**, respectively. When the temperature was adjusted, the final products didn't present any crystallinity. It is noteworthy that 2,2'-bipyridyl plays a critical role in the formation of **3b**, although 2,2'-bipyridyl is not present in compound **3b**. Control experiments show that if 2,2'-bipyridyl was

removed from reaction in the reaction system, the final products did not present any crystallinity, which indicate that 2,2'-bipyridyl plays a critical role in the formation of **3b**, although 2,2'-bipyridyl is not present in compound **3b**. Finally, the selection of suitable Cd(II) salts is the third crucial factor in synthesizing these compounds. Some other Cd(II) salts such as CdBr₂, CdI₂ and Cd(ClO₄)₂ were employed to replace CdCl₂ as the cadmium source in the reaction system of **3a**, and the final products present the same crystallinity as **3a**, but no crystals form in the reaction system of **3b**. Owing to this characteristic, CdCl₂ is selected as the reactant.

Structure of 1a. X-ray single crystal diffraction reveals that **1a** indicates a 3D framework crystallizing in the hexagonal space group *R*-3. It is interesting that 3D frameworks containing hexagonal channels and meso-helical chains (*P* + *M*) are observed in the structure of **1a**. The asymmetric unit of **1a** contains two crystallographically different TE ligands, one lattice water molecule and two Zn(II) cations, both of which adopt distorted trigonal bipyramidal coordination environment (Fig. 1a). The Zn1 cation is coordinated by three N atoms and two O atoms from three unique TE ligands. Of the five atoms, N1, O1, N8 and O2, adopting the bis-N,O-chelating coordination mode, are from two TE ligands, while the rest one [N4(a)] is from another crystallographically independent TE tetrazole ring. The Zn2 cation is five-coordinated by three N atoms and two O atoms from five different TE ligands and thus to form a nearly ideal [ZnN₃O₂] trigonal bipyramid constructed from two hydroxy oxygen atoms from two TE ligands, one tetrazole nitrogen atom from another QTZ ligand in the equatorial plane and two nitrogen atoms from other two crystallographically independent TE ligands located at the axial positions. The Zn-N and Zn-O bond lengths are in the range of 2.033(3)-2.248(3) Å and 1.953(2)-2.071(2) Å respectively. In compound **1a**, Each TE ligand adopts one single coordination mode (mode I in Scheme 2), acting as a quadridentate linker to connect four Zn cations. One pair of TE ligands incorporate one Zn1 and one Zn2 cations to form a repeat unit [Zn₂(TE)₂]. Simultaneously, two repeat units are interconnected via Zn2-TE coordination interactions to give a chain structure along *c*-axis as seen in Fig. 1b, with the separation of the adjacent being Zn1...Zn2 3.54 Å. As illustrated in Fig. 1c, such six chains constitute a unique metal-TE coordinated hexagonal channel via Zn1-TE coordination interactions containing a crystallographic 3-fold rotation axis along the *c*-axis as secondary building unit (SBU). Through the Zn2-TE coordination interactions, these SBUs are linked into 3D supramolecular framework (Fig. 1d). Meanwhile, water molecules are situated on the 3-fold rotation axes of hexagonal channels. It is interesting that two types of tube-like helical chains are generated between three arbitrary adjacent hexagonal SBUs, namely, right-handed *P* and left-handed *M*,

although they have the same components and linking sequence (Fig. S1). Each repeated helical unit includes two Zn atoms and one TE ligand with a helical pitch (Hp) of 6.77 Å, and the helix is generated from the crystallographic 3_1 axis. More interestingly, six infinitely right-handed and left-handed helical chains are arranged alternately around the hexagonal channels to form a 3D meso compound, where the neighboring Zn1 atoms of different helical chains are interlinked by the TE ligands (Fig. 1d). Obviously, the resulting complexes **1a** represents a very interesting example of 3D frameworks containing hexagonal channels and meso-helical chains (P + M) alternately trapped by the cooperative association of Zn1-TE coordination interactions in the solid state. To better understand of the nature of the intricate framework, a topological approach to simplification of 3D structures can be accomplished by reducing them to simple nodes and links. Therefore, if the $[\text{Zn}_2(\text{TE})_2]$ units are regarded as four connected nodes (Fig. 1e), the 3D framework of compound **1a** can then be seen in a simplified way as a *smd* net with point symbol $\{4^{11}.6^4\}$.

Structure of 1b. Structure determination indicates that compound **1b** possesses a 2D layered structure constructed from infinite organic chains and sulfate anions. The asymmetric unit of compound **1b** is shown in Fig. 2a, which crystallizes in an orthorhombic space group *Fdd2*. There are two Cd(II) cations, one TE ligand, one sulfate anion, one hydroxide anion, one coordination water molecule in an asymmetric unit. The two unique Cd(II) cations, Cd1 and Cd2, both have a distorted octahedral coordination geometry. The Cd-N bond lengths fall between 2.208 (4)-2.340 (3) Å and the Cd-O bond lengths range from 2.313 (7) to 2.461 (10) Å. Cd1 cation is coordinated by two oxygen atoms from two independent sulfate anions, two oxygen atoms from two hydroxide anions and two nitrogen atoms from two different TE ligands; Compared with Cd1 coordination geometry, there is only one oxygen atom from hydroxide anion as well as a coordinated water as a terminal ligand coordinated to Cd2 center. The sulfur sites show $[\text{SO}_4]$ tetrahedron geometry, which have one terminal oxygen atom and share three oxygen atoms with $[\text{CdN}_2\text{O}_4]$ octahedra (mode IX in Scheme 2). In the sulfate anions containing S1, the terminal S1-O6 distances are 1.451 (4) Å, whereas the bridging distances S1-O3,O4 and S1-O5 have bond distances of 1.476 (5) Å and 1.503 (3) Å, respectively. It is observed that the S-O bond lengths for oxygen atoms bound to $[\text{CdN}_2\text{O}_4]$ octahedra are longer than those of the terminal ones. The TE ligands are formally quadridentate, using four tetrazole nitrogen atoms N1, N2, N3, N4 coordinating to four different cadmium cations (mode II in Scheme 2). As can be seen from Fig. 2b, $[\text{CdN}_2\text{O}_4]$ octahedra share O7 corners from $\mu_3\text{-OH}^-$ anions with each other, and thus to form a chain with separation of the adjacent Cd1-Cd1 3.55 Å, which is reinforced by TE ligands to form a one-dimensional ribbon structure along *c*-axis.

Further, the adjacent ribbons are connected by sulfate anions via coordination bonds of O3, O4-Cd1 and O5-Cd1, Cd2 with the Cd-O distances ranging from 2.269(5) to 2.340(3) Å, which further consolidate the structure, leading to a two-dimensional wave-like layered structure through the *ac*-plane (Fig. 2c). All the sulfate anions act in the quadridentate bridging mode, using O3, O4 coordinated to two adjacent Cd1 cations in the same chains and O5 coordinated to two Cd2 cations from adjacent chains (mode IX in Scheme 2). Simultaneously, hexanuclear units [Cd₆S₂O₁₂] are generated between two adjacent ribbons (Fig. 2d). If the hexanuclear units [Cd₆S₂O₁₂] are considered as six connected nodes and the TE ligands as links, the 2D layer can be described as a *hxl* net (Fig. 2e). Furthermore, the strong O8—H8A...O4 and O8—H8B...O6 hydrogen bonds (Table S2) between adjacent layers assemble neighboring wavelike layers to form a 3D supra-molecular network along the *b* direction (Fig. 2f).

Structure of 2a. The single-crystal structure analysis of **2a** indicates a 3D framework crystallizing in the monoclinic space group *C* 2/*c*. The asymmetric unit contains two crystallographically independent Zn(II) cations, one TA ligand, one INA ligand and four lattice water molecule (Fig. 3a). The two categories of Zn(II) ions (Zn1 and Zn2) are in different coordination environments: Zn1 adopts distorted octahedral geometry, while Zn2 exhibits tetrahedron coordination geometry. The Zn1 cation is octahedrally coordinated by four N atoms and two O atoms from four unique TA ligands. Of the six atoms, N5, O4, N5(c) and O4(c), adopting the bis-N,O-chelating coordination mode, are from two TA ligands, while the rest two [N4(a), N4(b)] are from two other crystallographically independent TA tetrazole rings. The Zn2 atom is located on a general position, defined by two N atoms from one TA ligand and one INA ligand, two O atoms from two carboxylate groups of two unique INA ligands, respectively. The Zn–N bond lengths fall between 1.363(5)–2.206(3) Å and the Zn–O bond lengths range from 1.941(3) to 2.206(3) Å. In compound **2a**, all INA ligands are μ_2 -INA[−] anions which possess the same bridging coordination mode (mode X in Scheme 2). The TA ligands adopt one single coordination fashion (mode III in Scheme 2), acting as a quadridentate linker to chelate one Zn atom and bridges the other Zn atoms in a μ_4 -κN2:κN4:κO3:κN5, O4 coordination mode. Two Zn1 cations are joined together by a pair of TA ligands to form a [Zn₂(TA)₂] dimer with the Zn1...Zn1 distance of 4.25 Å (Fig. 3b). The [Zn₂(TA)₂] dimers are interconnected by sharing Zn1 cations in a perpendicular alternative arrangement, resulting in an undulating pearl-necklace-like chain running in the *bc*-plane (Fig. 3c). Simultaneously, each [Zn₂(TA)₂] dimer is further linked to the adjacent dimers in the same direction by sharing two Zn2 cations to form an infinite rod-shaped Zn-TA SBU along the *b*-axis (Fig. 3d).

Finally, the INA ligand linkers interconnect the Zn²⁺ metal ions from adjacent SBUs to construct a 3D network (Fig. 3e). The interlinked infinite rod-shaped SBUs are stacked in parallel and connected in the [110] directions by INA links to give one-dimensional (1D) rhombic channels of 8.4 Å along an edge and 12.4 Å along the diagonal into which four lattice water molecule per formula unit reside as guests. Despite there are plenty of INA ligands, the π,π -interactions does not occur obviously between the pyridine rings for the long distance of each other. However, hydrogen bonding (O(5)–H(5a)···O(2)) is in evident to further consolidate the gross structure. It is difficult to assign a topological network to this structure. Since a series of metal carboxylate coordination frameworks in terms of the packing and interconnection of 1D rods are proposed by Yaghi and O’Keeffe,⁴⁰ the whole structure of **2a** can also be described as an *sql* net when the rod-shaped Zn-TA SBUs are considered as finite four-connected nodes (Fig. 3f).

Structure of 2b. Compound **2b** represents an extremely rare example of incorporating both Cd_{1,2,3}-ligands rod-shaped SBUs and Cd_{4,5}-ligands 2D layer motifs in one tetrazolate coordination polymer. As revealed by single-crystal X-ray diffractions, Compound **2b** is a 3D structure and crystallizes in triclinic space group *P*-1. As displayed in Fig. 4a, the asymmetric unit of compound **2b** contains four and a half Cd(II) cations, three TA ligands and one azide anion, two independent hydroxide anions, two coordination and one lattice water molecules. All Cd(II) cations adopt slightly distorted octahedron coordination environments with the Cd–O distances being in the normal range of 2.226(4)–2.355(5) Å and Cd–N distance varying from 2.197(5) to 2.458(5) Å. Among the five unique Cd(II) cations, Cd1 center locates on an inversion center, so it is half-occupied in the asymmetric unit coordinated by two oxygen atoms of two carboxylate groups and two nitrogen atoms of two tetrazole rings from four different TA ligands, two oxygen atoms from two μ_3 -OH[−] anion; Cd2 adopts a [CdN₂O₄] coordination environment with the coordination sphere taken up by two oxygen atoms from two μ_3 -OH[−] anion and four atoms from two TA ligands, with N1, O1 atoms as well as N8g and O4g atoms being in a chelated fashion; Cd3 cation is surrounded by two nitrogen atoms and one oxygen atom from three different TA ligands, one oxygen atom from one OH[−] anion and two coordination water molecules; Cd4 cation are coordinated by three oxygen atoms of three carboxylate groups and one nitrogen atoms of one tetrazole ring from four different TA ligands, one oxygen atom from one μ_3 -OH[−] anion and one nitrogen atom from the azide anion; Cd5 cation is located on general position, defined by one O atom from one OH[−] anion, one N atom from the azide anion, and other four atoms. Of the four atoms, two O atoms are from two carboxylate groups of two different TA ligands while the rest two

N atoms are from two TA tetrazole rings of two other crystalgraphically independent TA ligands. In compound **2b**, TA ligand adopts two different coordination modes (mode IV, V in Scheme 2): Each TA ligand acts as a pentadentate linker to connect five Cd cations, respectively exhibiting $\mu_5\text{-}\kappa\text{N3}:\kappa\text{N4}:\kappa\text{O1}:\kappa\text{O2}:\kappa\text{O1,N1}$ (mode IV), $\mu_5\text{-}\kappa\text{N5}:\kappa\text{N6}:\kappa\text{O3}:\kappa\text{O4}:\kappa\text{N8,O4}$ (mode IV) and $\mu_5\text{-}\kappa\text{N9}:\kappa\text{N10}:\kappa\text{N12}:\kappa\text{O5}:\kappa\text{O6}$ (mode V) coordination mode. Whereas hydroxide ligand adopts the same type of coordination fashion: $\mu_3\text{-OH}^-$; and the azide anion acts a monodentate bridging coordination mode, using one nitrogen atom to link Cd4 center and Cd5 center (mode XI in Scheme 2). As shown in Fig. 4b, Cd2, Cd3 and Cd1 as well as Cd1 and Cd2A, Cd3A are strengthened by two $\mu_3\text{-O4}$ atoms to generate a pentanuclear $[\text{Cd}_5\text{O}_2]$ POM with the bond angle of Cd1-O4-Cd2, Cd1-O4-Cd3 and Cd2-O4-Cd3 being 103.83(18), 104.26(18) and 126.89(19) respectively, and the alternating $[\text{Cd}_5\text{O}_2]$ POM are offset and symmetry-related by an inversion Cd1 center. In the pentanuclear cluster unit, five Cd atoms are not on a plane, while Cd1, Cd2, Cd2A and two O7 atoms define an ideal parallelogram. Cd3 and Cd3A, above and below the parallelogram plane, respectively, graft onto the parallelogram by sharing $\mu_3\text{-O7}$. The pentanuclear units are linked together by TA ligands adopting mode I, each of which coordinates two different pentanuclear units. As shown in Fig. 4c, each pentanuclear unit is surrounded by four TA ligands, each pair of which connecting two pentanuclear units to form ‘double-bridges’.²⁹ As a result, each pentanuclear cluster unit is linked by two ‘double-bridges’, relating to two adjacent pentanuclear cluster units. With the alternating $[\text{Cd}_5\text{O}_2]$ POM connected by pairs of TA ligands, Cd1,2,3-ligands rod-shaped SBU in compound **2b** is constructed running along the *a*-axis. The formation of such an interesting rod-shaped SBU for **2b** constructed by pentanuclear $[\text{Cd}_5\text{O}_2]$ POMs and tetrazolate groups as ‘double-bridges’ may be ascribed to the unusual coordination mode of the TA ligand. It is noteworthy that Cd4 and Cd5 cations are alternatively bridged by $\mu_3\text{-OH}^-$ anions and azide ligands to construct the linear skeleton of a 1D chain running along the *a*-axis. And the skeleton is reinforced between adjacent Cd(II) cations to give the 1D chain in two ways: (i) by being bonded to four nitrogen atoms from two tetrazolate rings of two TA ligands; (ii) by being bonded to two amide groups of two TA ligands in bis-monodentate mode. Neighboring chains are further interconnected by TA ligands to give rise to the Cd4,5-ligands layer motif on crystallographic *ab*-plane (Fig. 4d). The Cd4,5-ligands layers, each having its N8, O4 atoms (from TA in mode II) chelating Cd2 cations whilst its N12 atoms (from TA in mode III) binding Cd3 cations of the Cd1,2,3-ligands chains to generate the 3D structure (Fig. 4e). The Cd4,5-ligands layers propagate along the *ab*-plane, while the Cd1,2,3-ligands chains propagate in the parallel direction along the *a*-axis. To the best of our knowledge, Compound **2b** represents a rare example of incorporating Cd1,2,3-ligands chains and

Cd_{4,5}-ligands layers in such an arrangement into one tetrazolate coordination polymer. It is noted that the structure of **2b** contains a [Cd₂O] dimer unit which is built by the interconnection Cd₄, Cd₅ cations and O₈ atom. From the topological point of view, both the [Cd₅O₂] POMs and [Cd₂O] dimer units can be regarded as 10-connected nodes. Thus, the overall structure of **2b** can be simplified as a 3D (10, 10)-connected net with {3¹⁴.4¹⁸.5¹¹.6²} {3¹⁷.4²¹.5⁷}₂ topology (Fig. 4f).

Structure of 2c. Compound **2c** represents a two-fold interpenetrating network constructed by the interconnection of numerous Zn–MT and Zn–INA chains, exhibiting the monoclinic space group *C* 2/c. As shown in Fig. 5a, in the asymmetric unit of **2c**, there are one crystallographically independent Zn(II) ion, one MT ligand, one INA ligand and one lattice water molecule. Each Zn (II) ion is coordinated in a slightly distorted tetrahedron with the coordination sphere taken by three nitrogen atoms from two different MT ligands and one INA ligand and one oxygen atom from carboxyl group of the MT ligand. The Zn–N and Zn–O bond lengths range from 1.958(3)–2.048(4) Å, and the N–Zn–N/O bond angles fall between 97.07(15)–121.05(15) °. The MT ligands acting in μ_2 - κ N1: κ N4 coordination mode are connected to two Zn(II) ions (mode VI in Scheme 2). Whereas the INA ligand is introduced in bridging coordination mode with the pyridine group and the carboxyl group each connecting one Zn(II) ion (mode X in Scheme 2). It is very interesting that the MT ligands ligate Zn(II) ions to form an infinite zigzag zinc chain running along the crystallographic *b*-axis (Fig. 5b). The Zn(II) centers are spanned by a MT ligand with a distance of 6.10 Å between each other. Such chains are interconnected through INA ligands roughly in the [0 1 1] direction to complete a 2D Zn–MT–INA honeycomb layer (Fig. 5c). The adjacent layers are pillared by INA linkers to form a 3D network (Fig. 5d). The single net of **2c** possesses large channels, which are able to be filled with solvents or be penetrated by another net in order to consolidate stability of the frameworks. In this case, two same 3D networks self-penetrate together to furnish a twofold interpenetration leaving only small cavities [a total of 576.8 Å³ (23.5 % of the total cell volume calculated by the PLATON program³⁰)] created by the formal removal of the uncoordinated water molecules. If the Zn(II) ions are considered as four-connected nodes and the MT and INA ligands both as linkers, the whole structure of compound **2c** can be described as a two-fold interpenetrating diamondoid net (Fig. 5e).

Structure of 3a. Crystal structure analysis revealed that compound **3a** crystallizes in the hexagonal system with space group *R*-3. As shown in Fig. 6a, there are one unique Cd(II), one BTMA anion and one lattice water molecule in the asymmetric unit in **3a**. The Cd(II) adopts the distorted

octahedral geometry surrounded by six nitrogen atoms from four BTMA anions with the Cd-N bond distances being 2.291(3) and 2.504(3) Å. In **3a**, there is only one type of BTMA anion, each BTMA anion adopts a $\mu_4\text{-}\kappa\text{N2}:\kappa\text{N4}:\kappa\text{N5}, \text{N6}, \text{N7}:\kappa\text{N9}$ bridging mode to link four cadmium atoms (mode VII in Scheme 2). Interestingly, the N4 and N5 atoms of BTMA anion bridge two metal atoms to construct a cyclic $[\text{Cd}_2(\text{BTMA})_2]$ dimer subunit (Fig. 6b). Further, each dimer subunit is surrounded by eight dimer subunits via the Cd-N9 and Cd-N2 bonds to form an infinite 3D framework (Fig. 6c and 6d). When viewed along the *c* axis, 1D hexagonal channels can be observed (Fig. 6d). From the topological view, if the dimer subunits are considered as eight-connected metal nodes, the structure of **3a** can be simplified as a 3D 8-connected framework with $\{4^4 \cdot 6^{16} \cdot 8^8\}$ topology (Fig. 6e).

Structure of 3b. Crystal structure determination revealed that compound **3b** also displays a 3D framework in the monoclinic crystal system of space group $P2_1/n$. In **3b**, the asymmetric unit contains two crystallographically independent Cd(II) centers that adopt different coordination environments, one TTMA ligand and one $\mu_3\text{-OH}$ anion (Fig. 7a). Cd1 is in a distorted octahedral geometry, coordinated by four nitrogen atoms from four TTMA anions and two oxygen atoms from two hydroxyl anions; Cd2 is also six-coordinated but by five nitrogen of three different TTMA anions and one oxygen atom of hydroxyl anion. The Cd-N bond lengths vary in the range of 2.311(9)-2.542(10) Å, and the Cd-O bond lengths vary from 2.277(7) to 2.298(7) Å, both falling into normal ranges. The coordination mode of TTMA anion in **3b** is shown in Scheme 2 (mode VI). It should be noted that the structure of **3b** contains tetranuclear $[\text{Cd}_4\text{O}_2]$ POMs (Fig. 7b), which are constructed through interconnection of Cd(II) cations by $\mu_3\text{-OH}$. Each tetranuclear Cd(II) unit is surrounded by eight TTMA anions (Fig. 7c), and each TTMA anion is connected to four tetranuclear $[\text{Cd}_4\text{O}_2]$ POMs (Fig. 7d). In this way, the TTMA anions link the tetranuclear units to form a 3D framework (Fig. 7e). From the topological point of view, the tetranuclear $[\text{Cd}_4\text{O}_2]$ POMs can be defined as 8-connected nodes, the organic ligands can be regarded as 4-connected nodes. Thus, the overall structure of **3b** can be simplified as a 3D (4, 8)-connected framework with $\{4^{10} \cdot 6^{14} \cdot 8^4\} \{4^5 \cdot 6\}_2$ *alb* topology (Fig. 7f).

Structural Diversity Tuned by Changing *In Situ* Generated Tetrazole Ligands From the Same Nitriles

In our synthesis, the cyanoacetamide failed to react to get the 2-(1H-tetrazol-5-yl)-acetamide but was instead *in situ* hydrolyzed to (1H-Tetrazol-5-yl)-acetic acid (TA) in **2a** and **2b**, as well as further *in situ* reduced to 5-methyl-tetrazole (MT) in **2c** (Scheme 3). Due to the different *in situ*

generated tetrazole ligands, the structure changes from 3D frameworks containing infinite rod-shaped SBUs in **2a** to two-fold diamondoid network in **2c**. Compared the structure of compound **3a** with **3b**, two different tetrazole ligands were also obtained with different reaction mechanism. One was bis-(1H-tetrazol-5-ylmethyl)-amine, the other was tris-(1H-tetrazol-5-ylmethyl)-amine. The change of *in situ* generated ligands resulted in dramatically structural divergence from a 3D 8-connected framework based on cyclic $[\text{Cd}_2(\text{BTMA})_2]$ dimer subunits to a 3D (4,8)-connected framework based on tetranuclear $[\text{Cd}_4\text{O}_2]$ POMs. The BTMA anion was prepared only by hydrothermal *in situ* [2+3] cycloaddition. But the *in situ* formation of TTMA anion was very different which may involve both *in situ* [2+3] cycloaddition and nucleophilic addition. In order to get insight into the mechanism, comparative experiments were carried out, which showed that **3b** was only available in the presence of 2,2'-bipyridyl under 180°C with aid of CdCl_2 . Although an exact mechanism is unclear at present, the main steps for the TTMA anion are proposed based on the common knowledge of nitriles, nucleophilic substitution³¹ and the ESI-MS spectrum (Fig. 8) in negative mode for the obtained filtrate of the *in situ* reaction (Scheme 4). First, the reaction starts with $\text{N}(\text{CH}_2\text{CN})_2$ ion obtained from protonation and expulsion of volatile HN_3 in the aid of NaN_3 .³² Second, the nucleophile $\text{N}(\text{CH}_2\text{CN})_2$ ion undergoes nucleophilic substitution with $\text{HN}(\text{CH}_2\text{CN})_2$ to form $\text{N}(\text{CH}_2\text{CN})_3$, and bond cleavage of the leaving group $\text{H}_2\text{NCH}_2\text{CN}$ was occurred at the same time. Then, $\text{H}_2\text{NCH}_2\text{CN}$ is hydrolyzed to produce $\text{H}_2\text{NCH}_2\text{COOH}$. The single at m/z 75.49 of the ESI-MS spectrum is in agreement with glycine. Finally, the TTMA anion was synthesized by *in situ* [2+3] cycloaddition reaction of $\text{N}(\text{CH}_2\text{CN})_3$ and NaN_3 with the aid of CdCl_2 . However, due to the complexities involved in the *in situ* ligand synthesis and supermolecular assemblies, it is difficult to explain the exact reaction mechanism in the one-pot, black-box-like hydrothermal metal/ligand reactions.³³

Thermal Stability and Powder X-ray diffraction (PXRD)

To study the thermal stability, thermogravimetric analyses of **1-3** were performed from 35 to 750 °C at a heating rate of 10 °C/min in dry air atmosphere. As shown in Fig. S2 to S4 (ESI[†]), for compound **1a**, the weight loss begins at 100 °C and one lattice water molecule is evacuated (calc./found: 5.02/5.01%) before 370 °C. Above 370 °C, the framework starts to decompose. For compound **1b**, one coordinated water molecule was removed from 100 to 230 °C (calc./found: 3.83/3.99%). The framework starts to collapse at about 230 °C. For compound **2a**, four lattice water molecules were removed from 35 to 319 °C (calc./found: 20.79/20.60%). The framework starts to

collapse at about 319 °C. Compound **2b** gradually loses one lattice and two coordination water molecules from 35 to 290 °C (calc./found: 5.34/5.67%) and the weight loss upon further heating is due to the collapse of the coordination polymer. Compound **2c** loses one lattice water from 100 to 310 °C (calc./found: 6.24/6.13%) and decomposes above 310 °C. The TGA curves of **3a** and **3b** indicate that they are stable up to approximately 290°C and 320°C, respectively. Above these temperatures, their networks start to decompose. A first weight loss for compound **3a** occurs between room temperature and 290°C, corresponding to the loss of interstitial water molecules (calc./found: 6.17/6.25%). And upon further heating, the weight losses are due to the decomposition of organic ligands and backbone collapse of the coordination polymer. PXRD measurements were carried on the compounds **1-3** to confirm the purity of these coordination polymers. The Simulated PXRD patterns are in fairly good agreement with the experimental patterns (Fig. S5 to S11, ESI[†]), which clearly confirms the phase purity of the as-synthesized products.

Photoluminescence

It is universally acknowledged that metal coordination frame-works with a d^{10} configuration possess excellent luminescence property.^{34, 35, 21e} The solid-state emission spectra of the complexes **1-3**, have been studied at room temperature, as shown in Fig. 9-11. The emission spectra have broad peaks with maxima at 406, 426, 439, 435, 457, 452 and 455 nm for compounds **1-3**, respectively, with the excitation upon 340 nm for **1a**, 360 nm for **1b**, 360 nm for **2a**, 349 nm for **2b**, 324 nm for **2c**, 396 nm for **3a** and 397 nm for **6**. As we know, it is usually believed that the energy transition of d^{10} complexes can be assigned as metal-to-ligand charge transfer, intraligand emission and ligand-to-metal charge transfer. From reported literatures, the free tetrazole ligand presents a very weak photoluminescence emission centered at 325 nm at room temperature.³⁶ Therefore, the strong fluorescence emission and distinct red-shift may be ascribed to the cooperative effects of intraligand emission and ligand-to-metal charge transfer (LMCT).^{36,37} The emission of **1** (406-426 nm) is blueshifted relative to the emissions of **2-3** (435-457 nm), which may be due to the long flexible hydroxyethyl chains with stronger vibrations of the frameworks and more radiationless energy decay. The variations of photoluminescence of these compounds may be attributed to the difference in the substituting groups at the 5-position of the tetrazole ligands to zinc/cadmium metal ions and/or their local coordination environments. In other words, the emissions can be tuned upon different ligands to same metal coordination environments (see **1a**, **2a** and **2c**; **1b**, **2b**, **3a** and **3b**), as well as the cluster-based metal ions.³⁸ These emission bands in the blue region suggest that these complexes may be potential candidates as blue-light emitting materials.

Nonlinear optical properties

The nonlinear optical (NLO) properties of the compound **2b** have also been investigated. The second harmonic generation experimental result shows that compound **2b** has SHG intensity of 0.5 versus that of urea, which confirms its acentric symmetry.³⁹

Conclusion

In summary, we have successfully isolated seven novel 3D and 2D metal-organic coordination polymers based on zinc and cadmium metal cations with different tetrazole ligands. All compounds exhibit diverse intriguing frameworks: Compound **1a** represents a very interesting example of 3D frameworks containing hexagonal channels and meso-helical chains (P + M) alternately trapped by Zn-TE coordination interactions; Compound **1b** possesses a 2D layered structure constructed from infinite organic chains and sulfate anions; Compounds **2a** and **2b** both crystallize in 3D frameworks containing infinite rod-shaped SBUs; Compound **2c** displays a two-fold diamondoid network. Compound **3a** shows a 3D framework consisting of cyclic $[\text{Cd}_2(\text{BTMA})_2]$ dimer subunits, possessing a 8-connected network topology; Compound **3b** shows a 3D binodal (4,8)-connected net based on tetranuclear $[\text{Cd}_4\text{O}_2]$ POMs as nodes. It is noteworthy that tuning the hydrothermal synthesis conditions, either changing pH or temperature, is a key step in the formation of coordination polymers with unexpected tetrazolate ligands. This observation is fascinating and this type of adaptation in the design of tetrazole coordination polymers has never been addressed to date.

Acknowledgements

This work was supported by the National Natural Science Foundation of China (21171060), the Program for New Century Excellent Talents in University (NCET-12-0643), the Natural Science Foundation of Guangdong Province (S2013010012678) and the High-Level Personnel Project of Guangdong Province in 2013.

References

- 1 (a) X. Y. Wu, Q. K. Zhang, X. F. Kuang, W. B. Yang, R. M. Yu and C. Z. Lu, *Dalton Trans.*, 2013, **41**, 11783; (b) W. C. Song, Q. Pan, P. C. Song, Q. Zhao, Y. F. Zeng, T. L. Hu and X. H.

- Bu, *Chem. Commun.*, 2010, **46**, 4890; (c) M. O’Keeffe and O. M. Yaghi, *Chem. Rev.*, 2012, **112**, 675; (d) S. M. Cohen, *Chem. Rev.*, 2012, **112**, 970; (e) J. P. Zhang, Y. B. Zhang, J. B. Lin and X. M. Chen, *Chem. Rev.*, 2012, **112**, 1001; (f) S. T. Zheng, T. Wu, C. Chou, A. Fuhr, P. Y. Feng and X. H. Bu, *J. Am. Chem. Soc.*, 2012, **134**, 4517; (g) H. Furukawa, N. Ko, Y. B. Go, N. Aratani, S. B. Choi, E. Choi, A. O. Yazaydin, R. Q. Snurr, M. O’Keeffe, J. Kim and O. M. Yaghi, *Science*, 2010, **329**, 424.
- 2 (a) G. F. Han, G. X. Wang, C. J. Zhu, Y. Cai and R. G. Xiong, *Inorg. Chem. Commun.*, 2008, **11**, 652; (b) R. Peng, M. Li and D. Li, *Coord. Chem. Rev.*, 2010, **254**, 1; (c) T. Hang, D. W. Fu, Q. Ye and R. G. Xiong, *Cryst. Growth Des.*, 2009, **9**, 2026; (d) T. Wen, D. X. Zhang and J. Zhang, *Cryst. Growth Des.*, 2013, **52**, 12; (e) J. R. Li, J. Sculley and H. C. Zhou, *Chem. Rev.* 2012, **112**, 869.
- 3 (a) V. A. Ostrovskii and A. O. Koren, *Heterocycles.*, 2000, **53**, 1421; (b) M. M. Harding and G. Mokdsi, *Curr. Med. Chem.*, 2000, **7**, 1289.
- 4 (a) X. L. Sun, Z. J. W, S. Q. Z, W. C. Song and C. X. Du, *Cryst. Growth Des.*, 2012, **12**, 4431; (b) P. Lama, E. C. Sanudo and P. K. Bharadwaj, *Dalton Trans.*, 2012, 2979.
- 5 (a) T. Y. Luo, H. L. Tsai, S. L. Yang, Y. H. Liu, R. D. Yadav, C. C. Su, C. H. Ueng, L. G. Lin and K. L. Lu, *Angew. Chem., Int. Ed.*, 2005, **44**, 6063; (b) M. Dincă and J. R. Long, *J. Am. Chem. Soc.*, 2007, **129**, 11172.
- 6 (a) Z. P. Demko and K. B. Sharpless, *J. Org. Chem.*, 2001, **66**, 7945; (b) Z. P. Demko and K. B. Sharpless, *Org. Lett.*, 2001, **3**, 4091; (c) Z. P. Demko and K. B. Sharpless, *Angew. Chem., Int. Ed.*, 2002, **12**, 2110; (d) F. Himo, Z. P. Demko, L. Noodleman and K. B. Sharpless, *J. Am. Chem. Soc.*, 2002, **124**, 12210; (e) F. Himo, Z. P. Demko, L. Noodleman and K. B. Sharpless, *J. Am. Chem. Soc.*, 2003, **125**, 9983.
- 7 (a) J. D. Ranford, J. J. Vittal, D. Wu and X. Yang, *Angew. Chem., Int. Ed.*, 1999, **38**, 3498; (b) C. Y. Xu, Q. Q. Guo, X. J. Wang, H. W. Hou and Y. T. Fan, *Cryst. Growth Des.*, 2011, **11**, 1869; (c) X. J. Wang, T. H. Huang, L. H. Tang, Z. M. Cen, Q. L. Ni, L. C. Gui, X. F. Jiang and H. K. Liu, *CrystEngComm*, 2010, **12**, 4356; (d) D. A. McMorran, *Inorg. Chem.*, 2008, **47**, 592; (e) D. R. Xiao, E. B. Wang, H. Y. An, Y. G. Li and L. Xu, *Cryst. Growth Des.*, 2007, **7**, 506; (f) Y. Zhang, L. Jianmin, M. Nishiura, W. Deng and T. Imamoto, *Chem. Lett.*, 1999, 1287; (g) J. D. Radford, J. J. Vittal and D. Wu, *Angew. Chem., Int. Ed.*, 1998, **37**, 1114.
- 8 (a) H. Zhao, Z. R. Qu, H. Y. Ye and R. G. Xiong, *Chem. Soc. Rev.*, 2008, **37**, 84; (b) D. C. Zhong, J. B. Lin, W. G. Lu, L. Jiang and T. B. Lu, *Inorg. Chem.*, 2009, **48**, 8656; (c) W. C. Song, Q. H. Pan, P. C. Song, Q. Zhao, Y. F. Zeng, T. L. Hu and X. H. Bu, *Chem. Commun.*, 2010, **46**,

- 4890.
- 9 (a) G. S. Yang, M. N. Li, S. L. Li, Y. Q. Lan, W. W. He, X. L. Wang, J. S. Qin and Z. M. Su, *J. Mater. Chem.*, 2012, **22**, 17947; (b) Q. P. Lin, T. Wu, S. T. Zheng, X. H. Bu and P. Y. Feng, *J. Am. Chem. Soc.*, 2012, **134**, 784.
- 10 (a) Y. B. Wang, D. S. Liu, T. H. Pan, Q. Liang, X. H. Huang, S. T. Wu and C. C. Huang, *CrystEngComm*, 2010, **12**, 3886; (b) J. Z. Liao, D. C. Chen, F. Li, Y. Chen, N. F. Zhuang, M. J. Lin and C. C. Huang, *CrystEngComm.*, 2013, **15**, 8180.
- 11 (a) X. L. Tong, T. L. Hu, J. P. Zhao, Y. K. Wang, H. Zhang and X. H. Bu, *Chem. Commun.*, 2010, **46**, 8543; (b) D. Kari, O. Wayne, P. Andrey, F. Steven, K. R. Dunbar and Z. Jon, *Cryst. Growth Des.*, 2012, **12**, 2662; (c) F. Yang, B. Y. Li, W. Xu, G. H. Li, Q. Zhou, J. Hua, Z. Shi and S. H. Feng, *Inorg. Chem.*, 2012, **51**, 6813.
- 12 (a) D. Braga, S. d' Agostino, E. D' Amen and F. Grepioni, *Chem. Commun.*, 2011, **47**, 5154; (b) H. C. Fang, J. Q. Zhu, L. J. Zhou, H. Y. Jia, S. S. Li, X. Gong, S. B. Li, Y. P. Cai, P. K. Thallapally, J. Liu and G. J. Exarhos, *Cryst. Growth Des.*, 2010, **10**, 3277.
- 13 R. B. Zhang, J. L. Zhao, J. K. Cheng, Y. Y. Qin, J. Zhang and Y. G. Yao, *Cryst. Growth Des.*, 2008, **8**, 2562.
- 14 (a) Y. C. Qiu, Y. H. Li, G. Peng, J. B. Cai, L. M. Jin, L. Ma, H. Deng, M. Zeller and S. R. Batten, *Cryst. Growth Des.*, 2010, **10**, 1332; (b) L. Ma, Y. C. Qiu, G. Peng, J. B. Cai and H. Deng, *Eur. J. Inorg. Chem.*, 2011, 3446; (c) L. Sun, L. Ma, J. B. Cai, L. Liang and H. Deng, *CrystEngComm.*, 2012, **14**, 890; (d) C. J. Zhao, C. W. Li, M. Y. Shen, L. F. Huang, Q. H. Li, M. Y. Hu and H. Deng, *Inorg. Chem. Commun.*, 2014, **48**, 30; (e) R. T. Dong, C. W. Li, M. Y. Shen, L. F. Huang, Q. H. Li, M. Y. Hu and H. Deng, *CrystEngComm.*, 2015, **17**, 1305.
- 15 J. Z. Liao, H. Ke, J. J. Liu, Z. Y. Li, M. J. Lin, J. D. Wang and C. C. Huang, *CrystEngComm*, 2013, **15**, 4830.
- 16 (a) X. M. Chen and M. L. Tong, *Acc. Chem. Res.* 2007, **40**, 162; (b) X. M. Zhang, *Coord. Chem. Rev.*, 2005, **249**, 1201; (c) L. Liang, C. F. Yang, Y. Z. Ma and H. Deng, *CrystEngComm*, 2013, **15**, 365.
- 17 (a) R. K. Feller, P. M. Forster, F. Wudl and A. K. Cheetham, *Inorg. Chem.*, 2007, **46**, 8717; (b) C. M. Liu, S. Gao and H.-Z. Kou, *Chem. Commun.*, 2001, 1670.
- 18 (a) J. Wang, Y. H. Zhang, H. X. Li, Z. J. Lin and M. L. Tong, *Cryst. Growth Des.*, 2007, **7**, 2352; (b) L. Han, X. Bu, Q. Zhang and P. Feng, *Inorg. Chem.*, 2006, **45**, 5736; (c) S. M. Humphrey, R. A. Mole, J. M. Rawson and P. T. Wood, *Dalton. Trans.*, 2004, 1670.
- 19 (a) X. M. Zhang and R. Q. Fang, *Inorg. Chem.*, 2005, **44**, 3955; (b) Y. Yan, C. D. Wu and C. Z.

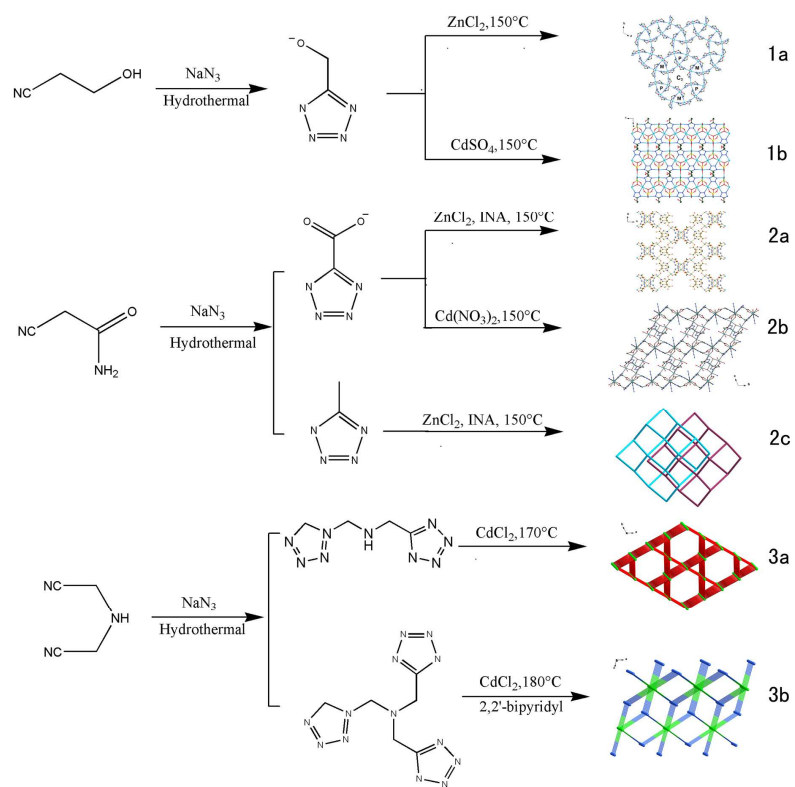
- Lu, Z. *Anorg. Allg. Chem.*, 2003, **629**, 1991.
- 20 (a) O. R. Evens and W. B. Lin, *Acc. Chem. Res.*, 2002, **35**, 511; (b) C. D. Wu, P. Ayyappan, O. R. Evens and W. B. Lin, *Cryst. Growth Des.*, 2007, **7**, 1690.
- 21 (a) H. Deng, Y. C. Qiu, Y. H. Li, Z. H. Liu, R. H. Zeng, M. Zeller and S. R. Batten, *Chem. Commun.*, 2008, 2239; (b) Y. C. Qiu, H. Deng, J. X. Mou, S. H. Yang, M. Zeller, S. R. Batten, H. H. Wu and J. Li, *Chem. Commun.*, 2009, 5415; (c) Y. C. Qiu, H. Deng, S. H. Yang, J. X. Mou, C. Daiguebonne, N. Kerbellec, O. Guillou and S. R. Batten, *Inorg. Chem.*, 2009, **48**, 3976; (d) L. Liang, G. Peng, L. Ma, L. Sun, H. Deng, H. Li and W. S. Li, *Cryst. Growth Des.*, 2012, **12**, 1151; (e) L. Ma, N. Q. Yu, S. S. Chen and H. Deng, *CrystEngComm*, 2013, **15**, 1352.
- 22 Y. L. Yao, L. Xue, Y. X. Che and J. M. Zheng, *Cryst. Growth Des.*, 2009, **9**, 606.
- 23 J. A. W. Harings, O. V. Asselen, R. Graf, R. Broos and S. Rastogi, *Cryst. Growth Des.*, 2008, **8**, 3323.
- 24 (a) R. L. Reeves and L. K. J. Tong, *J. Am. Chem. Soc.* 1962, **84**, 2050; (b) A. V. Tsymbal, M. D. Kosobokov, V. V. Levin, M. I. Struchkova and A. D. Dilman, *J. Org. Chem.*, 2014, **79**, 7831; (c) C. Pooput, W. R. Dolbier and J. M. Médebielle, *Org. Chem.*, 2006, **71**, 3564.
- 25 (a) X. L. Tong, D. Z. Wang, T. L. Hu, W. C. Song, Y. Tao and X. H. Bu, *Cryst. Growth Des.*, 2009, **9**, 2280; (b) J. M. Lin, B. S. Huang, Y. F. Guan, Z. Q. Liu, D. Y. Wang and W. Dong, *CrystEngComm*, 2009, **11**, 329; (c) J. M. Lin, Y. F. Guan, D. Y. Wang, W. Dong, X. T. Wang and S. Gao, *Dalton Trans.*, 2008, 6165; (d) L. L. Zheng, H. X. Li, J. D. Leng, J. Wang and M. L. Tong, *Eur. J. Inorg. Chem.*, 2008, 213; (e) M. Friedrich, J. C. Gálvez-Ruiz, T. M. Klapötke, P. Mayer, B. Weber and J. J. Weigand, *Inorg. Chem.*, 2005, **44**, 8044; (f) Y. Zhang, J. Yang, Y. Yang, J. Guo and J. F. Ma, *Cryst. Growth Des.*, 2012, **12**, 4060.
- 26 (a) B. Liu, Y. C. Qiu, G. Peng, L. Ma, L. M. Jin, J. B. Cai and H. Deng, *Inorg. Chem. Commun.*, 2009, **12**, 1200; (b) P. Cui, Z. Chen, D. L. Gao, B. Zhao, W. Shi and Peng. Cheng, *Cryst. Growth Des.*, 2010, **10**, 4370.
- 27 Bruker. *APEXII software*, Version 3.1.2; Bruker AXS Inc, Madison, Wisconsin, USA, 2004. Sheldrick, G. M. *SHELXL-97, Program for X-ray Crystal Structure Refinement*; University of Göttingen: Göttingen, Germany, 1997.
- 28 A. L. Spek, *J. Appl. Crystallogr.*, 2003, **36**, 7.
- 29 (a) D. L. Long, A. J. Blake, N. R. Champness, C. Wilson and M. Schröder, *Angew. Chem., Int. Ed.*, 2001, **40**, 2443; (b) M. F. Wu, F. K. Zheng, A. Q. Wu, Y. Li, M. S. Wang, W. W. Zhou, F. Chen, G. C. Guo and J. S. Huang, *CrystEngComm*, 2010, **12**, 260.
- 30 (a) A. L. Spek, *PLATON*, A Multipurpose Crystallographic Tool, Utrecht University, Utrecht,

- 2005; (b) A. L. Spek, *Acta Crystallogr., Sect. D.* 2009, **65**, 148.
- 31 (a) M. Khairat and R. Ibne, *J. Chem. Educ.*, 1967, **44**, 89; (b) D. D. Sung, T. J. Kim and I. Lee, *J. Phys. Chem. A*, 2009, **113**, 7073.
- 32 L. M. Dennis and H. Isham, *J. Am. Chem. Soc.*, 1907, **29**, 216.
- 33 (a) X. M. Chen and M. L. Tong, *Acc. Chem. Res.*, 2007, **40**, 162; (b) X. M. Zhang, *Coord. Chem. Rev.*, 2005, **249**, 1201.
- 34 (a) Z. Li, M. Li, X. P. Zhou, T. Wu, D. Li and S. W. Ng, *Cryst. Growth Des.*, 2007, **7**, 1992; (b) L. Tian, Z. Niu, Z. Y. Liu, S. Y. Zhou and P. Cheng, *CrystEngComm*, 2013, **15**, 10094; (c) L. Sun, G. Z. Li, M. H. Xu, X. J. Li, J. R. Li and H. Deng, *Z. Anorg. Allg. Chem.*, 2012, **1200**, 29; (d) Z. F. Liu, M. F. Wu, F. K. Zheng, M. J. Zhang, J. Chen, Y. Xiao, G. C. Guo and A. Q. Wu, *CrystEngComm*, 2013, **15**, 7038.
- 35 (a) J. Q. Sha, J. W. Sun, C. Wang, G. M. Li, P. F. Yan, M. T. Li and M. Y. Liu, *CrystEngComm*, 2012, **14**, 5053; (b) L. Liang, C. F. Yang, Y. Z. Ma and H. Deng, *CrystEngComm*, 2013, **15**, 365.
- 36 X. W. Wang, J. Z. Chen and J. H. Liu, *Cryst. Growth Des.*, 2007, **7**, 1227.
- 37 (a) J. R. Li, Y. Tao, Q. Yu and X. H. Bu, *Chem. Commun.*, 2007, 1527; (b) Y. C. Qiu, H. Deng, S. H. Yang, J. X. Mou, M. Zeller, S. R. Batten, H. H. Wu and J. Li, *Chem. Commun.*, 2009, 5415.
- 38 (a) S. L. Zheng and X. M. Chen, *Aust. J. Chem.*, 2004, **57**, 703; (b) V. W.-W. Yam and K. K.-W. Lo, *Chem. Soc. Rev.*, 1999, **28**, 323; (c) V. W.-W. Yam, *Acc. Chem. Res.*, 2002, **35**, 555.
- 39 S. K. Kurtz and T. T. Perry, *J. Appl. Phys.*, 1968, **39**, 3798.
- 40 N. L. Rosi, J. Kim, M. Eddaoudi, B. Chen, M. O'Keeffe and O. M. Yaghi, *J. Am. Chem. Soc.*, 2005, **127**, 1504.

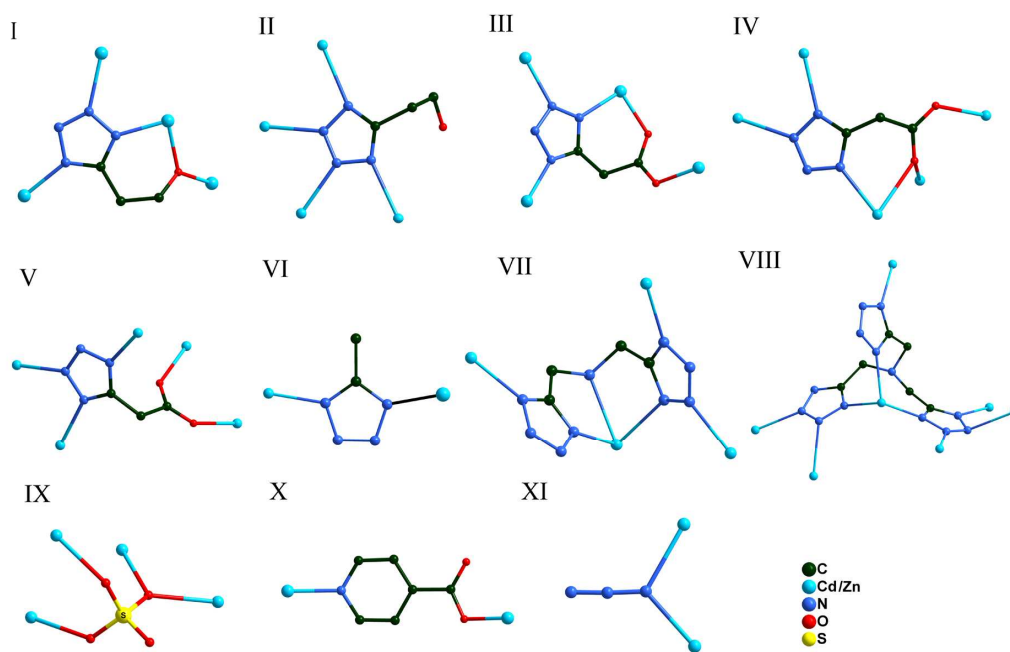
Table 1 Crystallographic data and structure refinement summary for complexes 1–3.

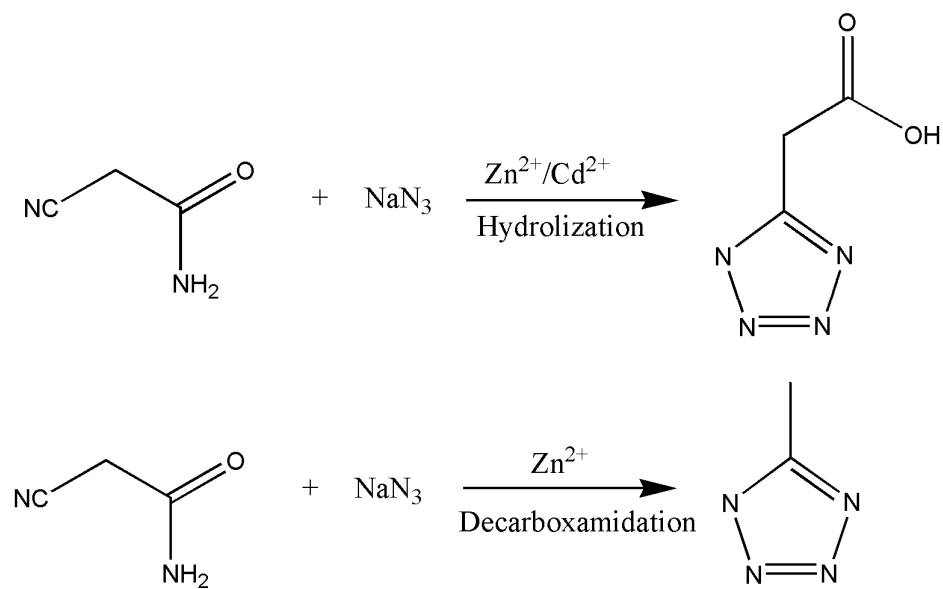
	1a	1b	2a	2b	2c	3a	3b
Formula	C ₁₈ H _{19.98} N _{2.2} O ₂ Zn ₆	C _{2.56} H ₇ Cd ₂ N ₄ O _{7.44} S	C ₁₈ H ₂₀ N ₁₀ O ₁₂ Zn ₃	C ₁₈ H _{23.66} Cd ₄ N ₁₀ O _{21.83}	C ₈ H ₉ N ₅ O ₃ Zn	C ₄ H ₅ CdN ₉ O ₂	C ₆ H ₇ Cd ₂ N ₁₃ O
Mr	1076.90	469.76	764.49	2021.26	288.57	323.58	502.07
Crystal system	hexagonal	orthorhombic	monoclinic	triclinic	monoclinic	hexagonal	Monoclinic
Space group	<i>R</i> -3	<i>Fdd</i> 2	<i>C</i> 2/ <i>c</i>	<i>P</i> -1	<i>C</i> 2/ <i>c</i>	<i>R</i> -3	<i>P</i> 21/ <i>n</i>
<i>a</i> (Å)	30.095(5)	17.501(3)	25.319(5)	7.3781(13)	16.852(2)	20.8197(13)	9.8747(8)
<i>b</i> (Å)	30.095(5)	33.436(6)	14.309(3)	13.574(2)	17.116(2)	20.8197(13)	6.7895(6)
<i>c</i> (Å)	6.7707(11)	7.1042(12)	7.0137(14)	13.578(2)	9.7103(14)	11.5581(15)	17.9044(15)
α (°)	90.00	90.00	90.00	113.181(2)	90.00	90	90
β (°)	90.00	90.00	96.379(3)	103.841(2)	118.683(2)	90	101.9580
γ (°)	120.00	90.00	90.00	90.00	90.00	120	90
<i>V</i> (Å ³)	5310.7(15)	4157.0(12)	2525.3(9)	90.952(2)	2457.2(6)	4338.8(7)	1174.34(17)
<i>Z</i>	6	16	4	1	8	18	4
<i>D</i> _c (g/cm ³)	2.020	3.002	1.821	2.787	1.560	2.009	2.840
μ (mm ⁻¹)	4.076	4.328	2.891	3.997	2.003	2.243	3.652
<i>F</i> (000)	3192.0	3549.8	1376.0	948.0	1168.0	2520	952
Goodness-of-fit	1.026	1.058	1.045	1.035	1.088	1.032	1.105
<i>R</i> 1 [<i>I</i> > 2 σ (<i>I</i>)] ^a	0.0363	0.0239	0.0326	0.0346	0.0453	0.0158	0.0488
<i>wR</i> 2 (all data) ^b	0.0945	0.0572	0.0730	0.0844	0.1601	0.0384	0.1183

$$^a R_1 = \frac{\sum ||F_0| - |F_c||}{\sum |F_0|}, \quad ^b wR_2 = \left\{ \frac{\sum [w(F_0^2 - F_c^2)^2]}{\sum (F_0^2)^2} \right\}^{1/2}$$

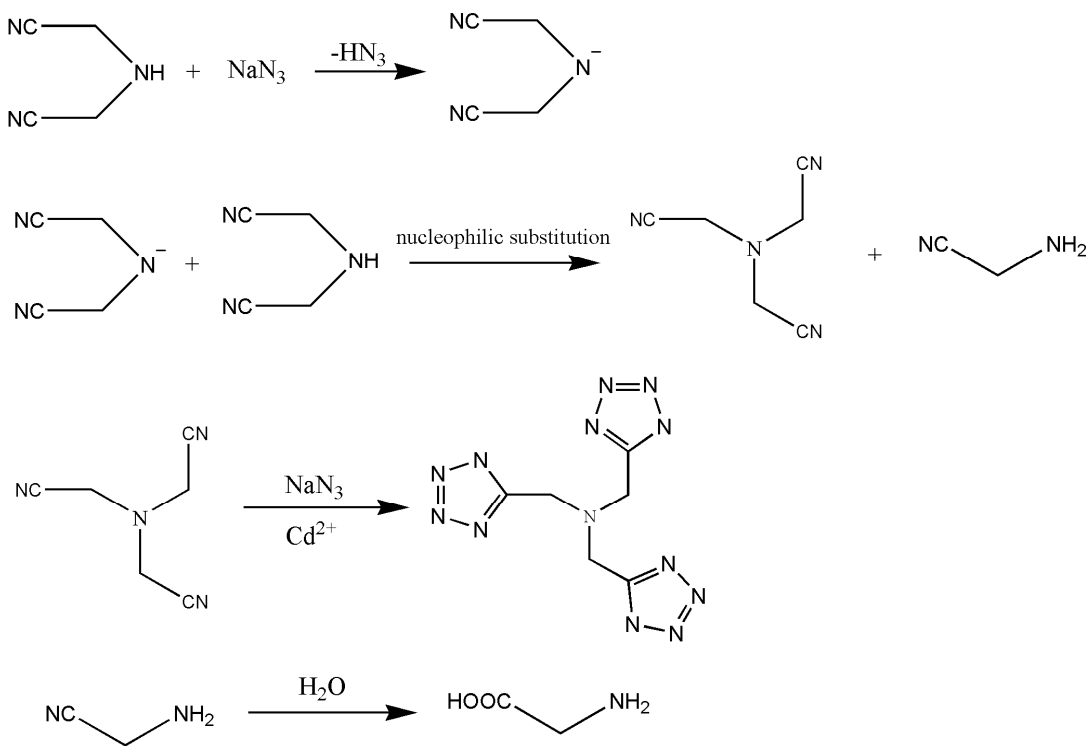
Scheme 1 *In Situ* Hydrothermal Syntheses of Compounds.

Scheme 2 Coordination modes of ligands.



Scheme 3 *In Situ* hydrolyzation and decarboxamidation reaction

Scheme 4 Possible pathway for Tris-(1H-tetrazol-5-ylmethyl)-amine from $\text{HN}(\text{CH}_2\text{CN})_2$, CdCl_2 and NaN_3 .



Figures and Captions

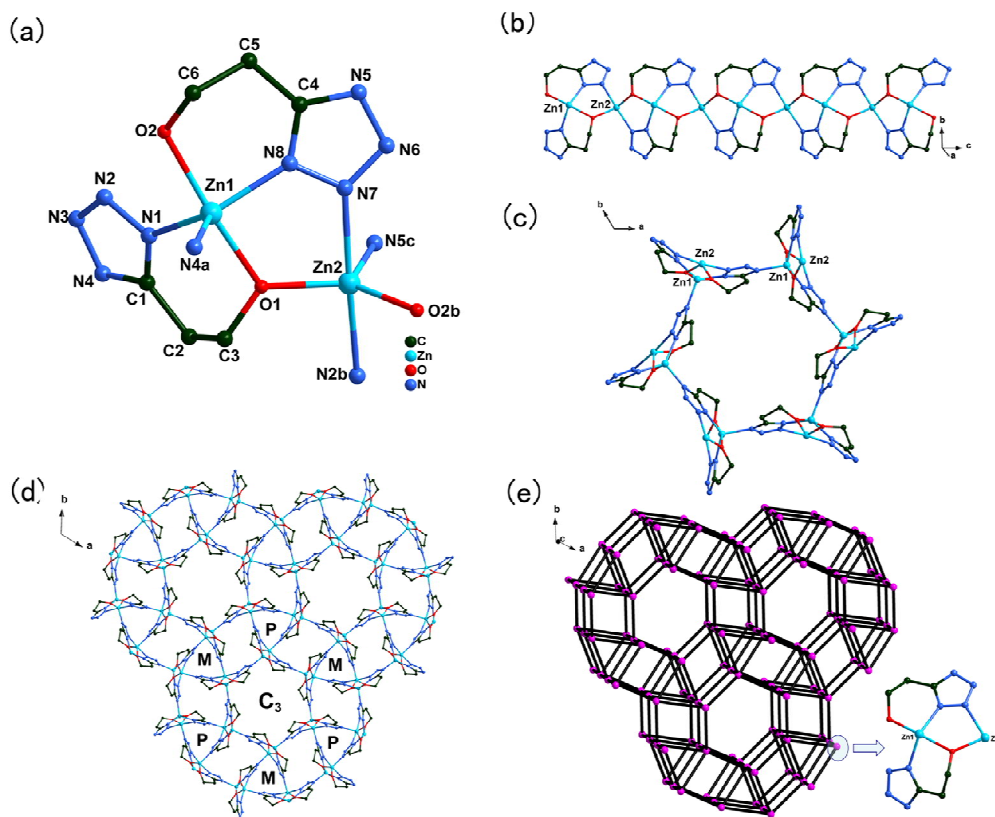


Fig. 1 (a). View of the coordination environment of the zinc ions. All H atoms and the solvent molecules are omitted for clarity. Symmetry code: a: $x - y, x, 1 - z$; b: $x, y, 1 + z$; c: $2/3 - y, 1/3 + x - y, 1/3 + z$. (b). View of the a 1D chain structure along c-axis constructed by $[Zn_2(TE)_2]$ units. (c). View of the hexagonal SBU along the c-axis. (d). View of 3D framework of compound **1a** formed by hexagonal SBUs along the c-axis. (e). View of the *smd* net of compound **1a**.

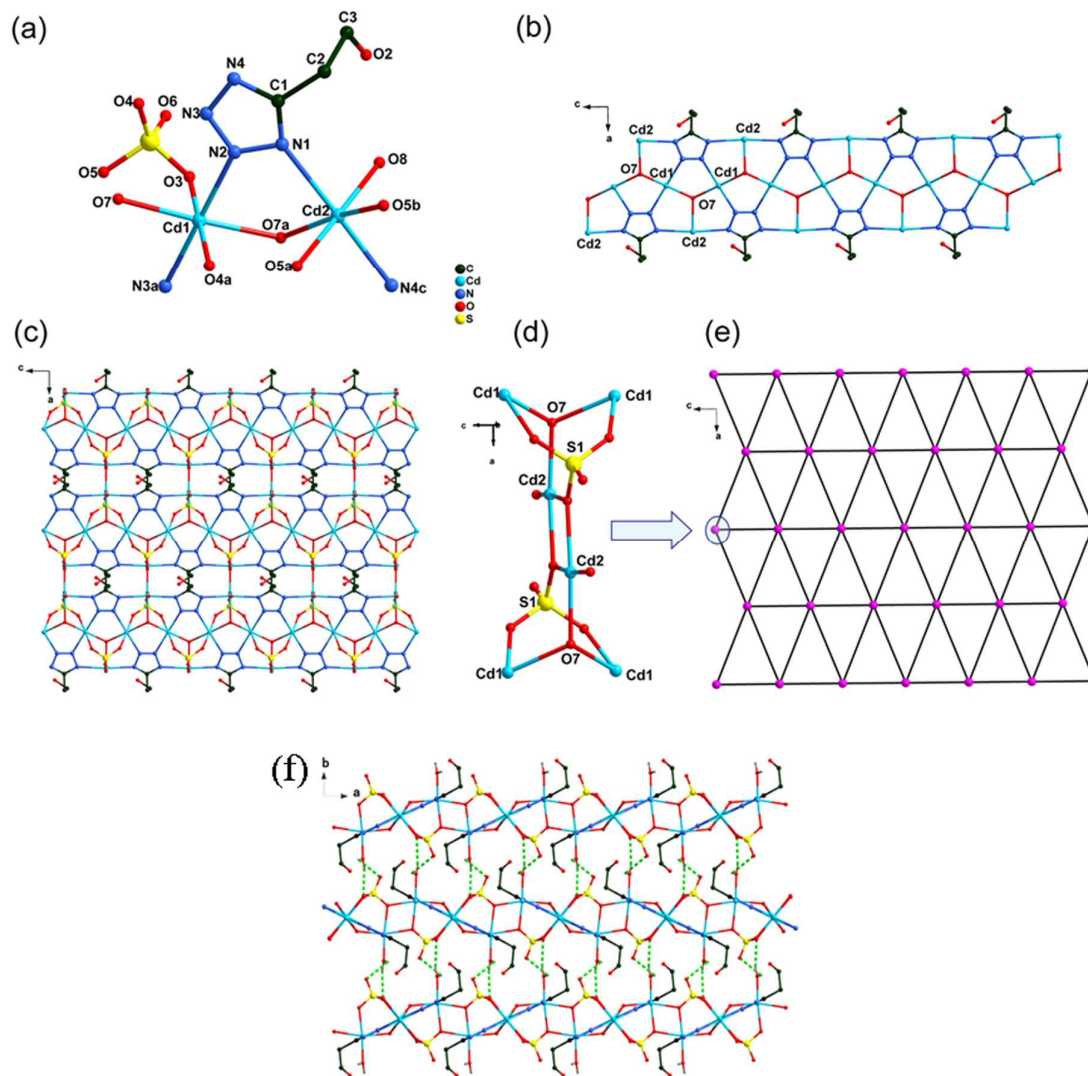


Fig. 2 (a). View of the coordination environment of the cadmium ions. All H atoms are omitted for clarity. Symmetry code: a: $0.5 - x, 2 - y, 0.5 + z$; b: $0.5 + x, y, 0.5 + z$; c: $x, y, 1 + z$. (b). View of the a 1D organic chain structure along *c*-axis. (c). View of the two-dimensional layered structure of **1b** constructed from infinite organic chains and sulfate anions through the *ac*-plane. (d). View of the hexanuclear units [Cd₆S₂O₁₂] generated between two adjacent ribbons. (e).View of the *hxl* net of compound **1b**. (f). View of the 3D supra-molecular network of **1b**.

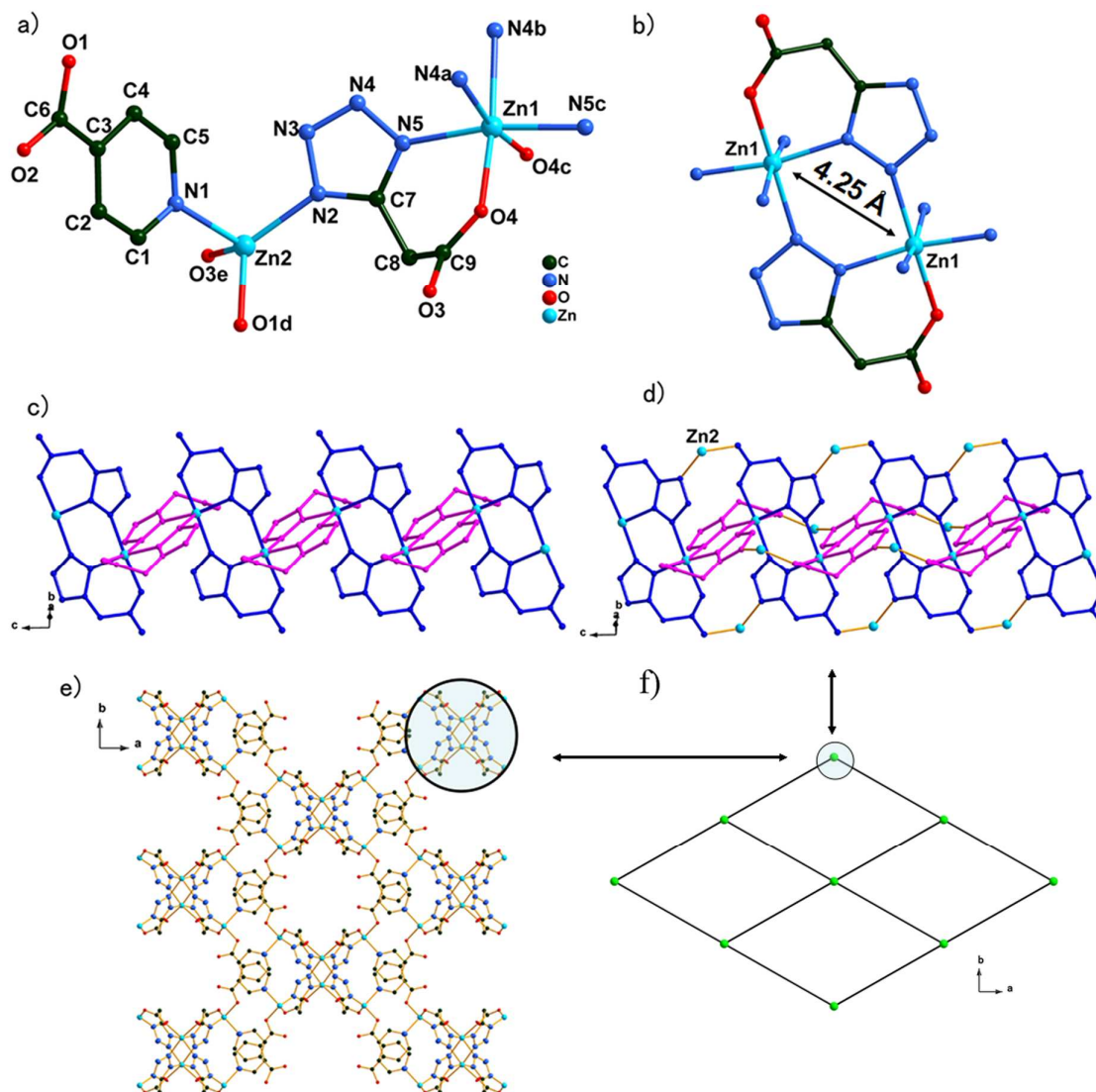


Fig. 3 (a). View of the coordination environment of the zinc ions. All H atoms are omitted for clarity. Symmetry code: a: $x, 1 - y, 0.5 + z$; b: $-x, 1 - y, 1 - z$; c: $-x, y, 1.5 - z$; d: $0.5 - x, 0.5 + y, 0.5 - z$; e: $x, y, -1 + z$. (b). View of the [Zn₂(TA)₂] dimer constructed by two Zn1 cations and a pair of TA ligands. (c). View of the pearl-necklace-like chain constructed by [Zn₂(TA)₂] dimers. (d). View of the rod-shaped Zn-TA SBU along the *b*-axis. (e). View of channels and 3D supramolecular framework of compound **2a** formed by Zn-TA SBUs and isonicotinate ions along the *c*-axis. (f) View of the *sql* type net when 1D rod-shaped Zn-TA SBUs are regarded as finite nodes.

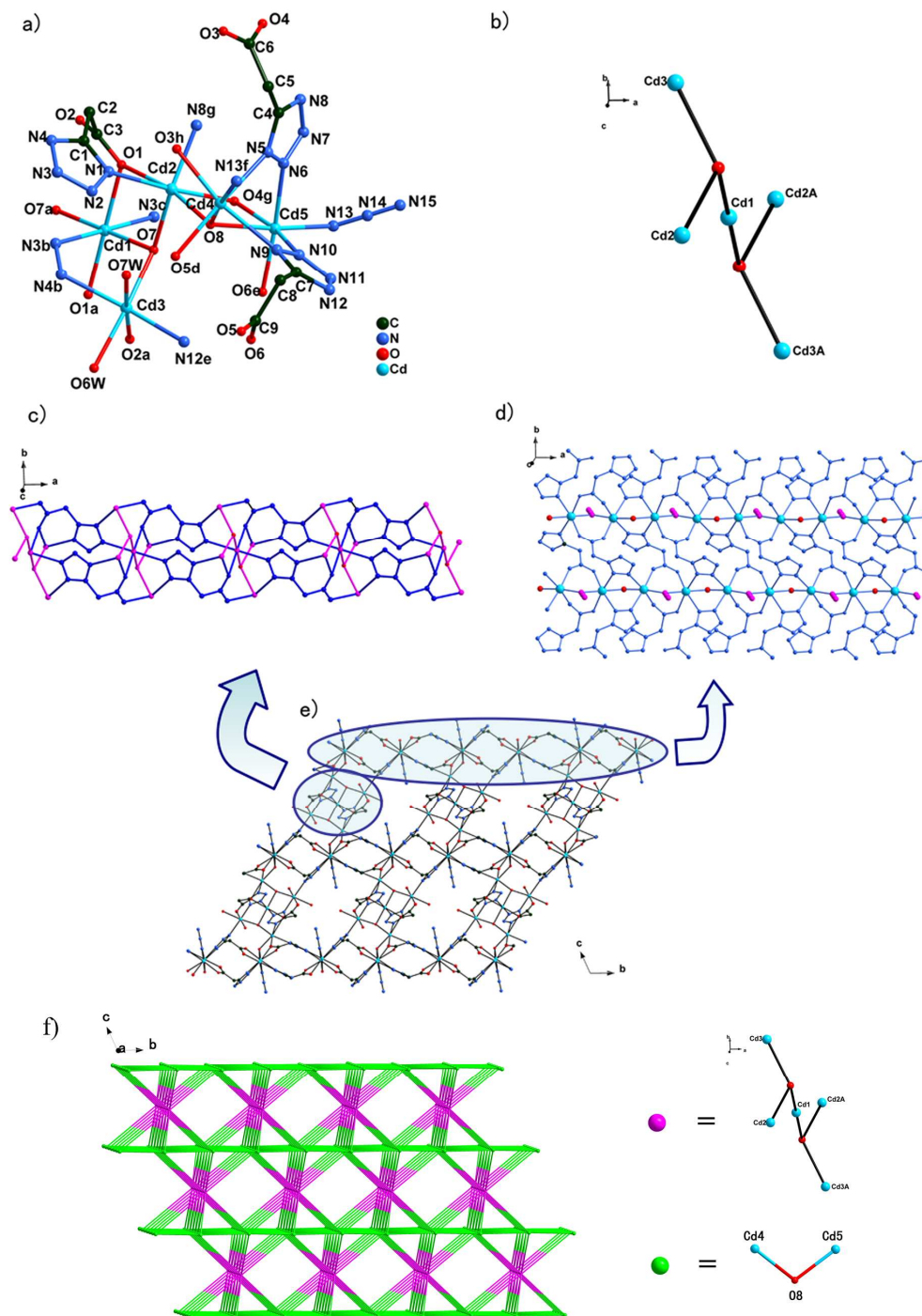


Fig. 4 (a) View of the coordination environment of the cadmium ions. All H atoms are omitted for clarity. Symmetry code: a: $1 - x, 1 - y, 1 - z$; b: $2 - x, 1 - y, 1 - z$; c: $-1 + x, y, z$; d: $2 - x, -y, -z$; e: $1 - x, -y, -z$; f: $1 + x, y, z$; g: $1 - x, 1 - y, -z$; h: $2 - x, 1 - y, -z$. (b) View of the pentanuclear $[Cd_5(\mu_3-OH)_2]$ unit. (c) View of the infinite Cd1,2,3-ligands rod-shaped SBU in Compound **2b** constructed by pentanuclear $[Cd_5(\mu_3-OH)_2]$ units and tetrazolate groups as 'double-bridges'. (d) View of the Cd4,5-ligands layer motif on crystallographic ab -plane. (e) View of the 3D structure constructed by Cd1,2,3-ligands chains and Cd4,5-ligands layers along the bc -plane. (f) View of the (10, 10)-connected net of **2b**.

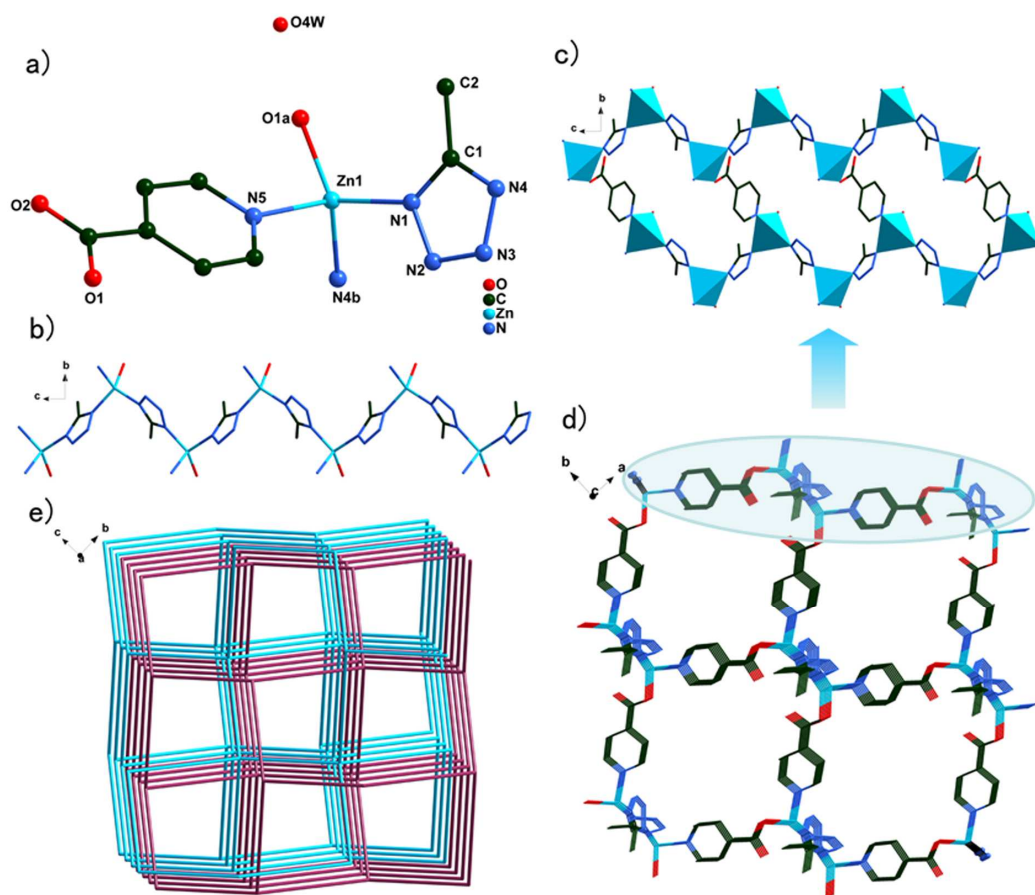


Fig. 5 (a) View of the coordination environment of the zinc ions. All H atoms are omitted for clarity. Symmetry code: a: $-0.5 + x, 0.5 - y, -0.5 + z$; b: $x, 1 - y, -0.5 + z$. (b) View of the infinite zigzag zinc chain constructed by the linkage of the Zn(II) centers and MT ligands along the *b*-axis. (c) View of the 2D Zn–MT–INA honeycomb layer along the *bc* plane. (d) View of the single 3D net of compound **2c**. (e) View of the two-fold diamond net of complex.

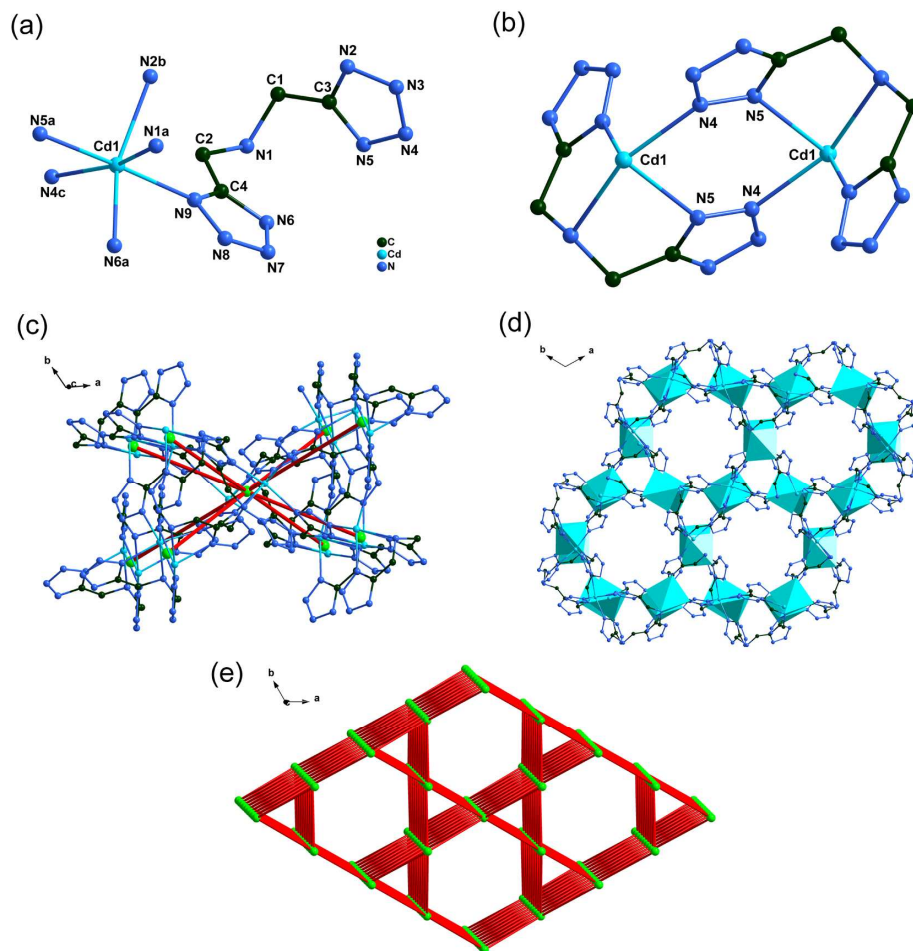


Fig. 6 (a). View of the coordination environment of the cadmium ions. All H atoms and the solvent molecules are omitted for clarity. Symmetry code: a: $-1/3 + y, 1/3 - x + y, 1/3 - z$; b: $-1/3 - x + y$; c: $4/3 - y, 5/3 + x - y, 2/3 + z$. (b) View of the cyclic $[\text{Cd}_2(\text{BTMA})_2]$ dimer subunits of **3a**. (c) Ball-and-stick diagram of a central 8-connected node surrounded by eight subunits, where the green balls represent the 8-connected nodes and the red sticks represent the connectivity between the nodes. (d) View of the 3D networks of **3a** assembled by cyclic $[\text{Cd}_2(\text{BTMA})_2]$ dimer subunits. (e) Schematic representation of the 8-connected topology with a point symbol of $\{4^4 \cdot 6^{16} \cdot 8^8\}$.

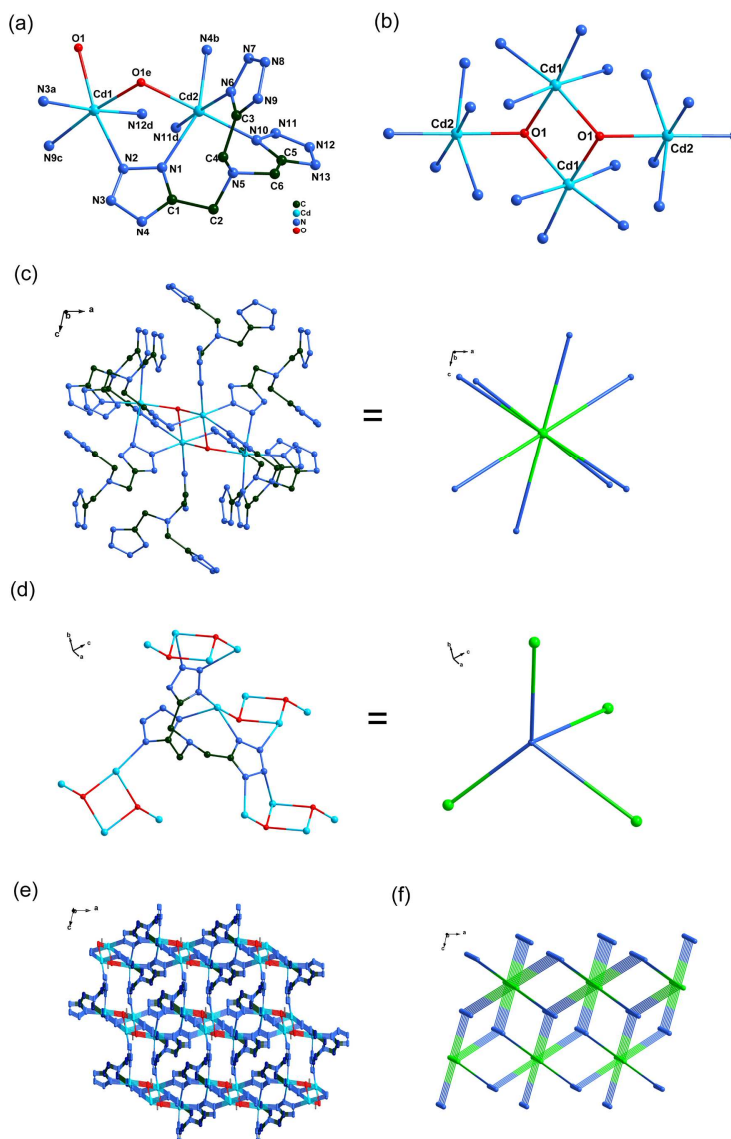


Fig. 7 (a). View of the coordination environment of the cadmium ions. All H atoms are omitted for clarity. Symmetry code: a: $2 - x, -y, 2 - z$; b: $x, 1 + y, z$; c: $0.5 + x, 0.5 - y, 0.5 + z$; d: $1 - x, 1 - y, 2 - z$; e: $2 - x, 1 - y, 2 - z$. (b) Coordination environment around metal center in tetranuclear $[\text{Cd}_4\text{O}_2]$ units. (c) 4-connected tetranuclear $[\text{Cd}_4\text{O}_2]$ POM node. (d) 4-connected TTMA anion node. (e) Ball-and-stick packing diagram of **3b** viewed along the crystallographic b -axis. (f) Schematic diagram of **3b** with alb net topology viewed along the approximate crystallographic b -axis.

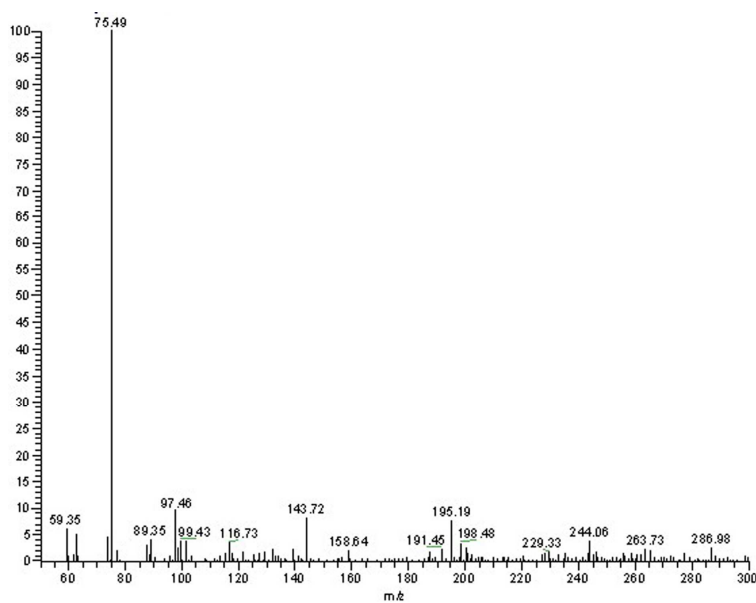


Fig. 8 The ESI-MS spectra for the obtained filtrate of **3b**.

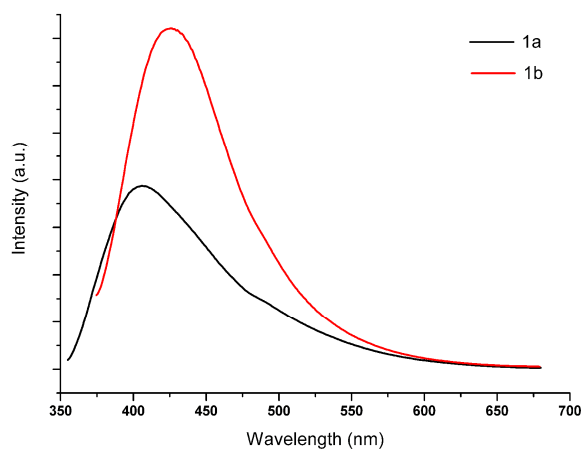


Fig. 9 Solid state emission spectra of **1a** and **1b** at room temperature

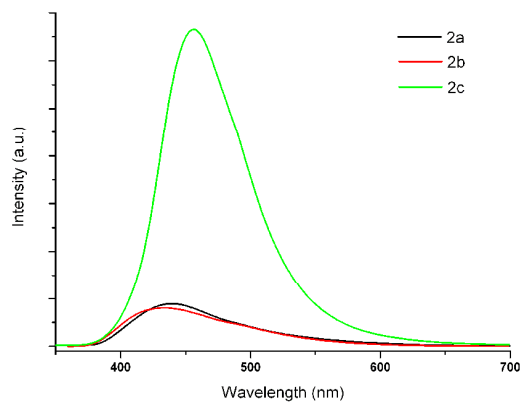


Fig. 10 Solid state emission spectra of **2a**, **2b** and **2c** at room temperature

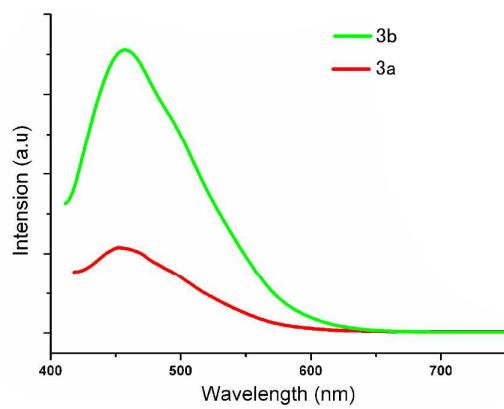


Fig. 11 Solid state emission spectra of **3a** and **3b** at room temperature